# Three-loop critical exponents, amplitude functions, and amplitude ratios from variational perturbation theory

H. Kleinert and B. Van den Bossche*
*Institut für Theoretische Physik, Arnimallee 14 D-14195 Berlin, Germany*
(Received 21 November 2000; published 18 April 2001)

We use variational perturbation theory to calculate various universal amplitude ratios above and below $T_c$ in minimally subtracted $\phi^4$ theory with $N$ components in three dimensions. In order to best exhibit the method as a powerful alternative to Borel resummation techniques, we consider only two- and three-loops expressions where our results are analytic expressions. For the critical exponents, we also extend existing analytic expressions for two loops to three loops.

DOI: 10.1103/PhysRevE.63.056113 PACS number(s): 64.60.−i

## I. INTRODUCTION

Recently, quantum mechanical variational perturbation theory [1] has been successfully extended to quantum field theory, where it has proven to be a powerful tool for determining critical exponents in three [2–4] as well as in $4-\epsilon$ dimensions [5,6]. The purpose of this paper it to apply this theory to amplitude ratios that can be measured experimentally. Their perturbation expansions suffer from the same asymptotic nature as those of the critical exponents, thus requiring delicate resummation procedures. These have been the subject of numerous studies, of that we can only mention a few, by various groups. There are two main approaches followed by various authors which we shall divide according to their method into a Paris school and a Parisi school.

The Paris school follows Wilson's ideas [7,8] by considering epsilon expansions in $D=4-\epsilon$ dimensions, making use of the fact that in the upper critical dimension $D_{\rm up}=4$ the theory is scale invariant. The results are at first power series in the renormalized coupling constant $g$. For small $\epsilon$, the coupling constant goes, in the critical limit of vanishing mass, to a stable infrared (IR) fixed point $g\rightarrow g^*$, where scaling laws are found [9]. The position of the fixed point is found as a power series in $\epsilon$ that makes critical exponents and amplitude functions likewise power series in $\epsilon$. These series diverge. The large-order behavior [10,11] suggests that these series are Borel summable [12,13]. The exact $\epsilon$ expansions of the critical exponents are known up to five loops [14,15]. They have been resummed with the help of Borel transformations and analytic mapping methods in Refs. [16–18].

The Parisi school follows Ref. [19] in studying perturbation expansions directly in $D=3$ dimensions [20–25]. In the original works, renormalization conditions are used according to which renormalized correlation functions should behave for small momenta like $G(p)\approx(p^2+m^2)^{-1}$. Recently, these normalization conditions have been replaced by dimensional regularization near $D=3$ to remove divergences (see, for instance, [23], which uses a regularization in $D=3-\varepsilon$ dimensions). Contrary to the $\epsilon$ expansions around $D_{\rm up}=4$, the system is not treated near the dimension of naive scale invariance, and the scaling properties are no longer obvious order by order in $g$. In addition, singular terms violating Griffith's analyticity are introduced that show up by amplitudes having unpleasant logarithmic dependences on the coupling constant.

The universal amplitude ratios were first discussed in [26] in the context of Wilson's renormalization group approach, and by Bervillier [27] within the field theoretic approach developed in [9]. The experimentally most easily accessible amplitude ratios are formed from the amplitudes of the leading power behaviors of various physical quantities in $T-T_c$ above and below the critical temperature $T_c$. A typical example, and one of the best measured amplitude ratios, is for the specific heat of superfluid helium above and below $T_c$. It was obtained in a zero-gravity experiment by Lipa *et al.* [28], who parametrized the specific heat as follows (we use the second of the references quoted in [28]):

$$C^{\pm}=\frac{A^{\pm}}{\alpha}|t|^{-\alpha}(1+D|t|^{\Delta}+E|t|^{2\Delta})+B,\quad t=T/T_c-1, \tag{1}$$

with $\alpha=-0.01056\pm0.0004$, $\Delta=0.5$, $A^+/A^-=1.0442\pm0.001$, $A^-/\alpha=-525.03$, $D=-0.00687$, $E=0.2152$, and $B=538.55$ (J/mol K). This parametrization is an approximation to the Wegner expansion form

$$F=F_{\pm}|t|^{\chi}(1+a_{0,1}|t|^{\Delta_0}+a_{0,2}|t|^{2\Delta_0}+a_{0,3}|t|^{3\Delta_0}+\cdots +a_{1,1}|t|^{\Delta_1}+a_{1,2}|t|^{2\Delta_1}+a_{1,3}|t|^{3\Delta_1}+\cdots) \tag{2}$$

with $\chi$ a combination of critical exponents and $F_{\pm}$ denoting the leading amplitude above and below $T_c$, respectively. Compared to this general Wegner expansion, higher powers in $\Delta_0\equiv\Delta$ have been neglected in Eq. (1), as well as daughter powers $\Delta_i, i\geqslant1$. This will be also the case in the present work, where we shall take into account only one exponent $\Delta$, related to $\omega$ by the relation $\Delta=\omega\nu$.

Further amplitude ratios are formed from the amplitudes $a_{i,j}$ of the nonleading power behaviors in $T-T_c$, the so-called confluent terms. Amplitude ratios of confluent terms are also universal quantities [25,29–31]. They are known up

*On leave from Physique Nucléaire Théorique, B5, Université de Liège Sart-Tilman, 4000 Liège, Belgium.

 ©2001 The American Physical Society

to five loops below $T_c$ [25] ($N=1$), or even up to six loops [30] ($N=1,2,3$) if only the $T>T_c$ regime is considered. ($N$ is the number of components of the field.) None of them will be examined here.

Apart from critical exponents and amplitude ratios, experimental observations show that the equation of state and the free energy have a simple scaling form of the Widom type, whose field-theoretic explanation can be found in various textbooks [9,12,13]. For example, the free energy of a system with magnetization $M_B$ may be represented near $T_c$ by $F(t,M_B)=|t|^{2-\alpha}f(|t|/M_B^{1/\beta})$, with $\alpha$ and $\beta$ being critical exponents and $t$ is the relative distance to the critical temperature. The scaling equation of state has been calculated in $\epsilon$ expansions to order $\epsilon^2$ for general O($N$) symmetry [32] and to order $\epsilon^3$ for the Ising model ($N=1$) [33].

### A. Perturbative calculation of amplitude ratios

Amplitude ratios relate the properties of the disordered phase, which are easy to calculate, to those of the ordered phase, which are much harder to derive. Several methods have been proposed to connect the two phases. One of them is due to Bagnuls and Bervillier [24], and was applied further in [25,34]. A similar procedure was followed in [22,23] for the amplitude ratio of correlation lengths, which had been omitted by Bagnuls and Bervillier. Calculations in three dimensions are usually numerical [20,24,25], although low orders can be treated analytically (see [22,23,34] for analytic three-loop results). Such analytic studies are important since they offer insight into the nonanalyticity with respect to the coupling constant. The amplitude ratio found in [22,23] is restricted to the Ising case $N=1$. The same is true for [35], which includes all diagrams up to three loops, as is the case of [34]. The latter work also incorporates a cubic anisotropic term, but for which the replica limit $N\rightarrow 0$ is considered, allowing to probe the critical behavior of the weakly dilute Ising system.

All power series are divergent and require resummation. Numerically, this has been done for the Ising model in [21] to five loops for the critical exponents, various amplitude ratios, and the equation of state. Reference [21] also contains comparisons between the results of different groups (both for $D=3$ and $D=4-\epsilon$), with experiments and with high-temperature series. For the most up-to-date work, see [18], which besides the critical exponents and amplitude ratios for the Ising model also gives the critical exponents for general O($N$) symmetry.

Another approach has been followed by Dohm and collaborators in Aachen [36–38] who proposed to use an analytic renormalization scheme in the form of minimal subtraction when working in $D=3$ dimensions. The use of the minimal subtraction scheme in field theories at fixed dimensions $2<D<4$ has one important advantage: the renormalization constants are the same in both the symmetric phase with $T>T_c$ and the ordered phase with $T<T_c$. The renormalization constants are power series in the renormalized coupling constant with coefficients that are poles in $\epsilon$ up to the given order of the perturbative series

$$Z=1+\sum_{i=1}^{L} a_i g^i, \quad a_i=\sum_{j=1}^{i} b_j \epsilon^{-j}. \tag{3}$$

The most important property of this scheme is that the mass does not enter explicitly the expansions, which can therefore be used on both side of $T_c$. Since the critical exponents are related to the renormalization constants, the mass independence of the $Z_i$ implies a clear decomposition of the correlation functions into amplitude functions and power parts. Working in three dimensions, there is a prize to pay: logarithmic singularities in the coupling constant. They can be removed using suitable length scales. This may be the physical length scale $\xi^+$ above $T_c$, and another length scale $\xi_-$ related, in the critical regime, to the longitudinal mass below $T_c$. Since they are not exactly equals, the Aachen group call the length scale $\xi_-$ a pseudolength. A precise definition of $\xi_-$ has been given in [36]. With different collaborators, Dohm has applied this scheme to derive various critical exponents and renormalization-group functions above $T_c$ [37], to calculate the heat capacity, the order parameter, and the superfluid density (both above and below $T_c$), as well as some useful universal combination of observable quantities [38]. So far, these works have been limited to low orders. The Ising model is the simplest system, since it contains no massless Goldstone modes that cause extra infrared singularities at intermediate stages of perturbative calculations of the thermodynamical quantities on the coexistence curve where the external magnetic field vanishes. The infrared singularities are the reason why the analytical equation of state and amplitude functions below $T_c$ have been restricted [27,38,39] to two loops for general $N$. These extra infrared singularities, which cancel at the end of the calculations, are caused by the physical singularities of the transverse susceptibility. Being physical, they remain at the end. Due to these difficulties, numerical studies up to five loops below $T_c$, with accurate Borel resummation are available only for the Ising case [21,25,40,41]. Only analytic three-loop calculations for the thermodynamic quantities below $T_c$ have become recently available for the general O($N$) system [42]. Based on these, calculations in which some contributions were evaluated up to five loops were done for amplitude ratios at $N=2$ and $N=3$ [41], proceeding as follows: Amplitude functions for the heat capacity were calculated using the three-loop result of [42] and five-loop results for the vacuum renormalization constant [41,43] and the critical exponent $\alpha$. For $\alpha$, use has been made of the values given in [17] for $N=1$, of the value given in the first of Ref. [28] for $N=2$ (this being the initial result of the space shuttle experiment, which was subsequently corrected), and of the value given in Ref. [44] for $N=3$. Since then, the works [2–6,13,18] have appeared and seem to be the best available references concerning resummed data. Although this is not the main subject of this paper, it is interesting to see in which way the new values of $\alpha$ affect the amplitude ratios of the heat capacity given in [41]. This will be done in Sec. IV.

In the following, we shall calculate amplitude ratios with the help of Kleinert's variational perturbation theory [1–6,13]. To exhibit the method most clearly, we shall base our study on analytical results only. This will restrict us to the level of three loops. Working at such low orders, the accuracy of our resummed values cannot compete with some existing five-loop calculations. For this reason, we shall not include nor discuss error bars in the final results.

To illustrate the method of variational perturbation theory, we shall first show how to obtain analytic expressions for the critical exponents, thus extending an earlier two-loop analytic calculation in Ref. [5]. After this, we apply the procedure to amplitude ratios of various experimental quantities. The critical exponents are computed directly from the renormalization constants of the theory. In the minimal subtraction scheme, the renormalization constants have only pole terms in $\epsilon$. For the amplitude functions, this is no longer true: in a $D=4-\epsilon$ approach, they have to be expanded in $\epsilon$. For this reason it is not *a priori* clear at which level the variational method has to be applied. For the purpose of showing the power of the method to resum amplitude ratios, it is then better to calculate amplitude ratios in three dimensions. A resummation of amplitude ratios within the $\epsilon$-expansion method is postponed to a later publication [45]. We shall also consider only the expansions of the Aachen group, especially their analytical two-loop [46] and three-loop [42] expansions. As a bonus, since the renormalization constants are the same (apart for trivial coefficients coming from the respective conventions) in the minimal subtraction scheme in $D=4-\epsilon$ dimensions and in fixed $D=3$ dimensions, the critical exponents will be the same in variational perturbation theory. This will be shown explicitly below.

The paper is organized as follows. In Sec. II, we define the model and the conventions. In Sec. III, we briefly review the strong-coupling approach and apply it to the evaluation of the critical exponents at the level of two and three loops, extending the results of Ref. [5]. Section IV is the main part of this paper, where we show how the strong-coupling limit of various amplitudes and amplitude ratios are determined. In Sec. IV F, we use the latest available value for the exponents $\alpha$ and $\nu$ [2–6,13,18] to calculate the amplitude ratio of the heat capacity and the universal combination $R_C$ (constructed from the leading amplitudes of the heat capacity, the order parameter, and the susceptibility above $T_c$), for $N=0,\ldots,4$, and to calculate the amplitude ratio of the susceptibilities in the Ising model ($N=1$). Finally, we draw our conclusion in Sec. V. For completeness, we have added an Appendix containing all formulas taken from other publications, and calculations related to them.

## II. MODEL AND CONVENTIONS

The critical behavior of many different physical systems can be described by an O($N$)-symmetric $\phi^4$-theory. In particular, the case $N=0$ describes polymers, $N=1$ the Ising transition (a universality class that comprises binary fluids, liquid-vapor transitions, and antiferromagnets), $N=2$ the superfluid helium transition, $N=3$ isotropic magnets (transition of the Heisenberg type), and $N=4$ phase transition of Higgs fields at finite temperature. In the presence of an external field $h_B$, the field energy is given by the Ginzburg-Landau functional

$$\mathcal{H}=\int d^Dx\left[\frac{1}{2}(\nabla\phi_B)^2+\frac{1}{2}r_0\phi_B^2+u_B(\phi_B^2)^2-h_B\cdot\phi_B\right]. \tag{4}$$

To facilitate comparisons with the results of Dohm and coworkers [42,46], we use the same normalizations. The fields $\phi_B$ and the external magnetic field $h_B$ have $N$ components, $u_B$ is the bare coupling constant, and $r_0$ a bare mass term, to be specified later. The integrals are evaluated in dimensional regularization. In dimension $D=3$, $\phi^4$-theory is superrenormalizable. This means that only a finite number of counterterms have to be added in order to make observables finite. More economically, the divergencies can be removed by a shift of the mass term and reexpanding in $r_0-r_{0c}$, where $r_{0c}$ is the critical value of $r_0$. In $\epsilon$-expansions, $r_{0c}$ vanishes. Near the critical temperature, $r_0$ behaves like $r_{0c}+a_0t$, where $t$ is the reduced temperature $(T-T_c)/T_c$. When working near $D=3$ dimensions, it is possible to use a simplified shift $\delta r_0$ that only contains the $D=3$ pole of $r_{0c}$ (and not the poles at $D_l>3$ with $l=3,4,5,\ldots$, where $D_l\equiv 4-2/l$). For convenience, we write the differences as a new mass term: $r_0-r_{0c}=m_B^2$ and $r_0-\delta r_0=m'^2_B$. In this way, we arrive at a new bare theory, with a mass term $m'^2_B$ that may be considered as the physical square mass of the theory. The introduction of the mass $m'_B$ makes the theory finite. It has, however, to be distinguished from the mass, field, and coupling-constant renormalization that still has to be performed: this latter renormalization, related to the introduction of the renormalization constants $Z_i$, is nothing else than a change of variables reflecting the fundamental scale-invariance hypothesis of the renormalization group approach. The distinction between the two steps—making the theory finite and renormalizing—is irrelevant in $D=4-\epsilon$ dimensions because $r_{0c}=0$ at $\epsilon=0$: Finiteness of the theory and the renormalization program are more intimately related than in $D=3$ dimensions. For a thorough discussion of the difference between the renormalization in $D=4-\epsilon$ and fixed $D=3$ dimensions, see [24,25], in particular p. 7215 in [24].

Within the minimal subtraction scheme, the renormalization constants $Z$, which are introduced to remove the poles at $D=4$, are given by

$$m_B^2=m^2\frac{Z_{m^2}}{Z_\phi}, \tag{5}$$

$$A_Du_B=\mu^\epsilon\frac{Z_u}{Z_\phi^2}u, \tag{6}$$

$$\phi_B=Z_\phi^{1/2}\phi, \tag{7}$$

the quantities on the right-hand side (rhs) being the renormalized ones. In Eq. (6), $\mu$ is an arbitrary reference mass scale and

$$A_D=\Gamma(1+\epsilon/2)\Gamma(1-\epsilon/2)\overline{S}_D,\quad \text{with}\quad \overline{S}_D=\frac{2\pi^{D/2}}{\Gamma(D/2)(2\pi)^D} \tag{8}$$

is a convenient geometric factor. The number $\bar{S}_D$ is equal to $S_D/(2\pi)^D$ where $S_D$ is the surface of a sphere in $D$ dimensions. Since $A_D$ goes to $\bar{S}_D$ when $D\to 4$, the renormalization constants have the same form [47] in $D=3$ as in $D=4-\epsilon$, and the resummation for the critical exponents is identical for the two approaches. This will be made clear below. For the amplitude calculations, however, things are different: If the expansions are truncated at some order, they turn out to depend on the difference between $A_D$ and $\bar{S}_D$. Rather than saying that the normalization of $A_D$ is a matter of convenience to simplify the $D$ dependence of lower order results [36,37], we shall see that the use of the geometric factor (8) improves low-order results: For example, the one-loop expansion of the amplitude function for the order parameter is identical to the zero-loop order [38].

With these conventions and notations, the renormalization constants in minimal subtraction are given up to three loops by [13–15]

$$Z_{m^2}=1+\frac{4(N+2)}{\epsilon}u+8(N+2)\left[\frac{2(N+5)}{\epsilon^2}-\frac{3}{\epsilon}\right]u^2+8(N+2)\left[\frac{8(N+5)(N+6)}{\epsilon^3}-\frac{4(11N+50)}{\epsilon^2}+\frac{31N+230}{\epsilon}\right]u^3, \tag{9}$$

$$Z_u=1+\frac{4(N+8)}{\epsilon}u+16\left[\frac{(N+8)^2}{\epsilon^2}-\frac{5N+22}{\epsilon}\right]u^2+\frac{8}{3}\left[\frac{24(N+8)^3}{\epsilon^3}-\frac{16(N+8)(17N+76)}{\epsilon^2}+\frac{96\zeta(3)(5N+22)+35N^2+942N+2992}{\epsilon}\right]u^3, \tag{10}$$

$$Z_\phi=1-\frac{4(N+2)}{\epsilon}u^2-\frac{8}{3}(N+2)(N+8)\left(\frac{4}{\epsilon^2}-\frac{1}{\epsilon}\right)u^3. \tag{11}$$

They are related to that in Ref. [13] by the replacement $u\to g/12$. This factor comes from the different coefficient of the coupling term $u\to g/4!$ in Eq. (4) and the fact that a factor $1/(4\pi)^2$ is absorbed in the definition of $g$ in [13], whereas a factor $A_{D=4}=1/(8\pi^2)$ is included here.

These renormalization constants serve to calculate all critical exponents including the exponent $\omega$ that characterizes the approach to scaling. This is the subject of Sec. III in which we illustrate the working of variational perturbation theory.

## III. EXACT CRITICAL EXPONENTS UP TO THREE LOOPS

Variational perturbation theory has been developed for the calculation of critical exponents in [2] and [5] in $D=3$ and $D=4-\epsilon$ dimensions, respectively. A review can be found in the textbook [13]. So we need to recall here only the main steps of the procedure.

Let $f_L(\bar{u}_B)$ be the partial sum of order $L$ of a power series

$$f\approx f_L(\bar{u}_B)=\sum_{i=0}^{L} f_i\bar{u}_B^i. \tag{12}$$

In the present context,

$$\bar{u}_B=u_B\mu^{-\epsilon}A_D \tag{13}$$

with $D=3$ and $\epsilon=1$, i.e., $\bar{u}_B=u_B/(4\pi\mu)$. The mass scale $\mu$ will be specified later. As seen from Eq. (6), this scale leads to a dimensionless coupling constant $\bar{u}_B$. We assume that in Eq. (12), the ultraviolet (UV) divergencies have been removed. In $D=3$ dimensions, this is achieved by working with $m_B^2$ instead of $r_0$. However, $r_{0c}$ is a nonperturbative quantity in three dimensions, and working with $m_B^2$ or $m'^2_B$ generates nonanalyticities due to the presence of logarithms of the coupling constant. These will be removed by the introduction of the correlation length $\zeta_+$ above $T_c$ and of the length $\zeta_-$ below $T_c$, see [38]. The mass scale $\mu$ will be identified with the inverse of these correlation lengths $\zeta_\pm^{-1}$ in the two phases. Since the correlation lengths go to infinity like $|t|^{-\nu}$ as the critical point is approached, the series has to be evaluated in the limit of an infinite dimensionless bare coupling constant $\bar{u}_B$. In the renormalization group approach, this regime is studied by mapping the expressions into a regime of finite renormalized quantities using the renormalization constants (5)–(7). If we can find directly the strong-coupling limit, this renormalization is avoidable. To understand this, consider the relation between the renormalized and the bare coupling constant at the one-loop order $u=u_B\mu^{-\epsilon}-c/\epsilon(u_B\mu^{\epsilon})^2$, where $c$ is a constant. At the critical point, $\mu\to 0$, or $\bar{u}_B\to\infty$, and the series expansion breaks down. If we sum a ladder of loop diagrams, we obtain $1/u=1/(u_B\mu^{-\epsilon})+c/\epsilon$. Now critical theory can easily be reached to give a renormalized $u^*=\epsilon/c$. A strong-coupling expansion in the bare coupling will turn out to give the same result. From our point of view, the renormalization group approach is simply a specific procedure of evaluating power series in the strong-coupling limit.

In $D=4-\epsilon$ dimensions, the situation is slightly more involved since renormalization is also necessary to obtain UV-finite quantities, the mass shift $r_0-r_{0c}$ not being sufficient for this goal as in the super-renormalizable case $D=3$, since $r_{0c}=0$ as $\epsilon\to 0$. As far as this paper is concerned, we shall make use of the fact that $D=3$ and $D=4-\epsilon$ dimensions series expansions in terms of renormalized quantities are available in the literature. These will be converted back to bare expansion, using the inverse of Eqs. (5)–(7). For $D=3$ dimensions, this expresses all physical quantities in powers of $u_B/\mu$. The mass scale $\mu$ is identified with $\zeta_\pm^{-1}$ in the disordered or ordered phase, respectively. In $D=4-\epsilon$ dimensions, the critical theory is obtained by identifying $\mu \to m$ with the renormalized mass $m$ in the disordered phase. In a subsequent publication [48], we will show how to perform directly a calculation in terms of UV-finite bare quantities in $D=4-\epsilon$. In this way, the renormalization procedure is superfluous, our sole problem being the evaluation of the expansions in the limit of infinite coupling constant.

Inverting Eq. (6), we have the expansion

$$u=\bar{u}_B\Bigg\{1-\frac{4(N+8)}{\epsilon}\bar{u}_B+8\left[\frac{2(N+8)^2}{\epsilon^2}+\frac{3(3N+14)}{\epsilon}\right]\bar{u}_B^2 -8\left[\frac{8(N+8)^3}{\epsilon^3}+\frac{32(N+8)(3N+14)}{\epsilon^2} +\frac{96\zeta(3)(5N+22)+33N^2+922N+2960}{3\epsilon}\right]\bar{u}_B^3\Bigg\}. \quad (14)$$

The expansion (14) has the same strong-coupling limit in $D=3$ and $D=4-\epsilon$ dimensions, and it does not matter that $\mu=\zeta_\pm^{-1}$ for $D=3$ or $\mu=m$ for $D=4-\epsilon$ since both quantities go to zero in the critical limit with the same power $|t|^{-\nu}$. With relation (14) between $u$ and $\bar{u}_B$, we obtain the bare coupling expansion of the renormalized square mass and fields:

$$m^2\equiv Z_r^{-1}m_B^2=m_B^2\Bigg\{1-\frac{4(N+2)}{\epsilon}\bar{u}_B+4(N+2)\times\left[\frac{4(N+5)}{\epsilon^2}+\frac{5}{\epsilon}\right]\bar{u}_B^2-16(N+2)\times\left[\frac{4(N+5)(N+6)}{\epsilon^3}+\frac{53N+274}{3\epsilon^2}+\frac{(5N+37)}{\epsilon}\right]\bar{u}_B^3, \quad (15)$$

$$\phi\equiv Z_\phi^{-1/2}\phi_B=\phi_B\left[1+\frac{2(N+2)}{\epsilon}\bar{u}_B^2-\frac{4}{3}(N+2)(N+8)\times\left(\frac{8}{\epsilon^2}+\frac{1}{\epsilon}\right)\bar{u}_B^3\right]. \quad (16)$$

These two expressions are sufficient to calculate the critical exponents $\nu$ and $\gamma$ and, via scaling relations, all other exponents. Note that the value of the renormalized coupling constant at the critical point $u^*$ is not needed to obtain $\nu$ and $\gamma$. The expansion (14) is, however, useful for obtaining an accurate exponent $\omega$ of the approach to scaling. It was pointed out in [49] that $\omega$ can also be deduced from the expansions of $\nu$ and $\gamma$. However, to reach the same accuracy, this requires always one more loop compared to the loop order we are interested in. For this reason, we shall take the advantage of Eq. (14), whose three-loop order contains all necessary information to get $\omega$ to that given order.

### A. Method

Starting from Eq. (12), we follow [2,5,13] to write its strong-coupling limit as

$$f_L(\bar{u}_B\to\infty)=\mathrm{opt}_{\hat{u}_B}\left[\sum_{i=0}^{L}f_i\hat{u}_B^i\sum_{j=0}^{L-i}\binom{-i\epsilon/\omega}{j}(-1)^j\right]. \quad (17)$$

The symbol $\mathrm{opt}_{\hat{u}_B}$ denotes optimization with respect to $\hat{u}_B$. This expression holds provided it yields a nonzero constant. This limit will be denoted by $f^*$:

$$f(\bar{u}_B\to\infty)=f^*+c_0\bar{u}_B^{-\omega/\epsilon}+O(\bar{u}_B^{-2\epsilon/\omega}), \quad (18)$$

where $c_0$ is a constant. The optimalization is supposed to make $f$ depend minimally on $\hat{u}_B$. In practice, this amounts to taking the first derivative to zero (odd orders) or, when it yields complex results, to taking the second derivative to zero and selecting turning points.

After having determined the optimum at various order $L$, it is still necessary to extrapolate the result to infinite order $L\to\infty$. The general large-$L$ behavior of the strong-coupling limit has been derived from an analysis in the complex plane in [2,13]:

$$f_L^*\approx f^*+c_1\exp(-c_2L^{1-\omega}), \quad (19)$$

with constants $c_1$ and $c_2>0$. Knowing this behavior, a graphical extrapolation procedure may be used to find $f_\infty^*=f^*$.

To apply the above algorithm to critical exponents, we proceed as follows: Let $W_L$ be a function obtained from perturbation theory. It has an expansion

$$W_L(\bar{u}_B)=\sum_{i=0}^{L}W_i\bar{u}_B^i. \quad (20)$$

Suppose that we also know this function has a leading power behavior $\bar{u}_B^{p/q}$ for large $\bar{u}_B$. The power $p/q$ is given by a logarithmic derivative

$$\frac{p}{q}=\frac{d\ln W_L}{d\ln\bar{u}_B}. \quad (21)$$

The right-hand-side is a power series representation of a function of the type (12), with $p/q$ being $f^*$ and the approach to $f^*$ in the form of powers $\bar{u}_B^{-\omega/\epsilon}$. Equation (21) will be used later for the determination of the critical exponents. If the series (20) goes to a constant in the strong-coupling limit, the exponent $p$ is vanishing, and we are left with

$$\frac{d\ln W_L}{d\ln\bar{u}_B}=0. \quad (22)$$

This equation can be solved for $q$, i.e., for $\omega$. Note that Eq. (21) strictly holds for $p\neq 0$. However, it can be shown that this equation may be used also for $p=0$, i.e., that Eq. (22) is a consistent equation for functions that go to a constant in the strong-coupling limit. This is explained in Appendix A. In the following, we shall directly use Eqs. (21) and (22) for two- and three-loop expansions where everything can be calculated analytically. We give below the associated formulas resulting from Eq. (17). Setting $\rho=1+\epsilon/\omega$, we find for $L=2$:

$$f^{*}_{L=2}=\mathrm{opt}_{\hat{u}_B}(f_0+f_1\rho\hat{u}_B+f_2\hat{u}_B^2)=f_0-\frac{\rho^2}{4}\frac{f_1^2}{f_2}, \tag{23}$$

while the three-loop results $L=3$ lead to

$$f^{*}_{L=3}=\mathrm{opt}_{\hat{u}_B}(f_0+\overline{f}_1\hat{u}_B+\overline{f}_2\hat{u}_B^2+f_3\hat{u}_B^3)$$
$$=f_0-\frac{1}{3}\frac{\overline{f}_1\overline{f}_2}{f_3}\left(1-\frac{2}{3}r\right)+\frac{2}{27}\frac{\overline{f}_2^3}{f_3^2}(1-r), \tag{24}$$

where $\overline{f}_1=f_1\rho(\rho+1)/2, \overline{f}_2=f_2(2\rho-1), r=\sqrt{1-3\overline{f}_1f_3/\overline{f}_2^2}$. If the square root is imaginary, the optimal value is given by the unique turning point. Practically, and this is a virtue of the analytic result, this square root is always imaginary for $D=3$, at least as for the exponent $\omega$. The turning point condition leads to

$$f^{*}_{L=3}=f_0-\frac{1}{3}\frac{\overline{f}_1\overline{f}_2}{f_3}+\frac{2}{27}\frac{\overline{f}_2^3}{f_3^2}, \tag{25}$$

i.e., to same expression as Eq. (24), but with $r=0$. In the case $D=4-\epsilon$ with $\epsilon\to 0$, $r$ is real. However, for $\omega$ the $\epsilon$-expansion of $r$ produces higher orders in $\epsilon$ than the three-loop approximation admits. Then, in both $D=3$ and the $\epsilon$-expansion, Eq. (25) is the relevant equation. A word of caution is, nevertheless, necessary: The positive root $r$ of

$$\hat{u}_B^{*}=\frac{f_2}{3f_3}(-1\pm r) \tag{26}$$

has to be chosen in order to match the three-loop result with the two-loop one in the limit $f_3\to 0$. Doing so, it must be assumed that $f_2$ and $f_1$ are nonvanishing. When optimizing with $f_2=0$, it is straightforward to show that if $f_1f_3>0$, then the optimum corresponds to $\hat{u}_B^{*}(f_2\to 0)=0$ and $f^{*}_{L=3}=f_0$. The other possibility, $f_1=0$, is also interesting since it occurs in the determination of the exponent $\eta$. It can be verified that $f_1=0$ implies taking the negative root $r=-1$, so that $\hat{u}_B^{*}(f_1\to 0)=-2\overline{f}_2/(3f_3)$ and $f_3^{*}=f_0+4\overline{f}_2^3/(27f_3^2)$. This possibility has not been discussed in the previous works [2,5,13].

### B. Critical exponents

After the introduction to the resummation method to be used in this work, we can now turn to the actual determination of the critical exponents. We start from the definitions within the conventional renormalization formalism of the functions

$$\gamma_m=\frac{\mu}{m^2}\frac{\partial m^2}{\mu}\bigg|_B, \tag{27}$$

$$\gamma_\phi=\mu\frac{\partial}{\partial\mu}\ln Z_\phi\bigg|_B, \tag{28}$$

$$\beta_u=\mu\frac{u}{\partial\mu}\bigg|_B, \tag{29}$$

which, in the critical regime $m_B^2\to 0$, render the critical exponents $\eta_m=\gamma_m^{*}$ and $\eta=\gamma_\phi^{*}$ if the first two equations are calculated at the fixed point $u^{*}$ determined by the zero of the third function $\beta_u$. The derivative of $\beta_u$ at $u^{*}$ is the critical exponent of the approach to scaling $\omega=\partial\beta_u/\partial u|_{u^{*}}$.

Using the relation between the bare coupling constant $u_B$ and the reduced one $\overline{u}_B$ given in Eq. (13), Eqs. (27) and (28) become

$$\eta_m=-\epsilon\frac{d}{d\ln\overline{u}_B}\ln\frac{m^2}{m_B^2}=-\epsilon\frac{d}{d\ln\overline{u}_B}\ln Z_r^{-1}, \tag{30}$$

$$\eta=\epsilon\frac{d}{d\ln\overline{u}_B}\ln\frac{\phi^2}{\phi_B^2}=2\epsilon\frac{d}{d\ln\overline{u}_B}\ln Z_\phi^{-1/2}, \tag{31}$$

where the renormalization constants $Z_r^{-1}$ and $Z_\phi^{-1/2}$ have been explicitly given up to three loops in Eqs. (15) and (16), respectively. The associated power series expansion in $\overline{u}_B$ of the exponents $\eta_m$ and $\eta$ will now be treated with the help of the formalism described in the previous section, up to two and three loops.

### C. Critical exponents from two-loop expansions

In order to calculate the two-loop expansions in the critical strong-coupling limit, we need to know $\omega$ to this order. This will be calculated from Eq. (14). Dividing this series by $\overline{u}_B$, we know that the leading power behavior as $\overline{u}_B\to\infty$ is $-1$ since $u$ is supposed to go to the constant value $u^{*}$: $u\overline{u}_B^{-1}|_{\overline{u}\to\infty}=u^{*}\overline{u}_B^{-1}$. Calculating the logarithmic derivative of Eq. (14) and expanding up to second order in $\overline{u}_B$, we have

$$\frac{d}{d\ln\overline{u}_B}\ln\frac{u}{\overline{u}_B}=\frac{-4(N+8)}{\epsilon}\overline{u}_B$$
$$+16\left[\frac{(N+8)^2}{\epsilon^2}+\frac{3(3N+14)}{\epsilon}\right]\overline{u}_B^2. \tag{32}$$

We now apply formula (A4). Combining with Eq. (23), we identify

$$-1=-\frac{\rho^2}{4}\frac{[-4(N+8)/\epsilon]^2}{16[(N+8)^2/\epsilon^2+3(3N+14)\epsilon]}, \tag{33}$$

i.e.,

$$\frac{\rho^2}{4}=1+3\epsilon\frac{3N+14}{(N+8)^2}, \tag{34}$$

from which we can deduce $\omega$:

$$\omega=\frac{\epsilon}{\rho-1}=\frac{\epsilon}{-1+2\sqrt{1+3\epsilon(3N+14)/(N+8)^2}}. \tag{35}$$

It is identical to the result obtained in [5]. As a check of Eq. (35), we verify that it reproduces the well-known $\epsilon$-expansion

$$\omega_\epsilon=\epsilon-3\epsilon^2(3N+14)/(N+8)^2. \tag{36}$$

We refer the reader to [5,13] for plots of the function (35) as $\epsilon$ goes from 0 to 1, and for a comparison with the unresummed $\epsilon$-expansion. The strong-coupling limit of $\omega$ may also be calculated from Eq. (A1) with an analytic expression different from Eq. (35), although numerically they are practically the same, and they certainly have the same $\epsilon$-expansion [49].

This determination of $\omega$ illustrates what we said in Sec. II, that in the minimal renormalization scheme the critical exponents lead to identical results in $D=3$ and $D=4-\epsilon$ dimensions. This will also be true for the critical exponents to be calculated in the sequel [50]. For this reason, we shall always keep track of $\epsilon$ to facilitate the comparison, although our work is in $D=3$ dimensions. Only for amplitude ratios to be calculated later will such a comparison be impossible and $\epsilon$ be set equal to 1 everywhere.

Knowing $\omega$, we can now determine the exponents $\eta$ and $\eta_m$. According to Eqs. (30) and (31), we take the logarithmic derivative of Eqs. (15) and (16), reexpand the results up to the second order in $\bar{u}_B^2$, and obtain

$$\eta_m=4(N+2)\bar{u}_B-8(N+2)\left[\frac{2(N+8)}{\epsilon}+5\right]\bar{u}_B^2, \tag{37}$$

$$\eta=8(N+2)\bar{u}_B^2. \tag{38}$$

Evaluating $\eta_m$ in the strong-coupling limit in the same way as $\omega$, i.e., following the algorithm (17), we find

$$\eta_m=\frac{\rho^2}{4}\,\frac{[4(N+2)]^2}{8(N+2)[2(N+8)/\epsilon+5]}$$
$$=\frac{(N+2)}{(N+8)+5\epsilon/2}\left[\epsilon+\epsilon^2\frac{3(3N+14)}{(N+8)^2}\right]. \tag{39}$$

For $\eta$, the situation is less clear. In [2,5], it was argued that the two-loop result cannot be computed from Eq. (38) since no linear term in $\bar{u}_B$ is present. A direct application of the resummation algorithm would give an optimum $\hat{u}_B^*=0$, then a value $\eta=0$ at two-loop order. This does not lead to the correct $\epsilon$-expansion, according to which the exponent starts with $\epsilon^2$, i.e., with a nonvanishing two-loop contribution. To apply variational perturbation theory, it is necessary to modify the procedure. In Ref. [5], this was done by considering a different critical exponent

$$\gamma=\nu(2-\eta), \tag{40}$$

with

$$\nu=\frac{1}{2-\eta_m}. \tag{41}$$

To obtain their strong-coupling limit, we insert for $\eta_m$ and $\eta$ their perturbative expansions (37) and (38), respectively, and reexpand the resulting ratios in power of $\bar{u}_B$ up to the second order. This gives

$$\gamma=1+2(N+2)\bar{u}_B-4(N+2)\left[\frac{2(N+8)}{\epsilon}-(N-4)\right]\bar{u}_B^2. \tag{42}$$

The critical exponent $\nu$ itself has the expansion

$$\nu=\frac{1}{2}+(N+2)\bar{u}_B-2(N+2)\left[\frac{2(N+8)}{\epsilon}-(N-3)\right]\bar{u}_B^2. \tag{43}$$

The strong-coupling limits are, using $\rho^2/4$ from Eq. (34),

$$\gamma=1+\frac{(N+2)}{2(N+8)-\epsilon(N-4)}\left[\epsilon+\epsilon^2\frac{3(3N+14)}{(N+8)^2}\right], \tag{44}$$

$$\nu=\frac{1}{2}\left\{1+\frac{(N+2)}{2(N+8)-\epsilon(N-3)}\left[\epsilon+\epsilon^2\frac{3(3N+14)}{(N+8)^2}\right]\right\}. \tag{45}$$

Their $\epsilon$-expansion are in agreement with $D=4-\epsilon$ results [5,13]. From these expressions we can recover $\eta$ using the relation $\eta=2-\gamma/\nu$. The result has now the correct $\epsilon$ expansion:

$$\eta=\frac{N+2}{2(N+8)^2}\epsilon^2. \tag{46}$$

This calculation of $\eta$ via $\nu$ and $\gamma$ was made in [2,5] to compensate the lack of a linear term in Eq. (38). Let us point out that, even if the $\epsilon$-expansion is not recovered, it is nevertheless hidden in a direct resummation of Eq. (38) to $\eta=0$. To see this, we add a small dummy linear term $\zeta u$, to the defining equation (31), leading to the expansion

$$\eta=\zeta\bar{u}_B+\left[8(N+2)-\zeta\frac{4(N+8)}{\epsilon}\right]\bar{u}_B^2. \tag{47}$$

Using Eqs. (23) and (34), this leads to the strong-coupling value

$$\eta=-\frac{\rho^2}{4}\,\frac{\zeta^2}{8(N+2)-4(N+8)\zeta/\epsilon}, \tag{48}$$

which is zero for $\zeta=0$. Consider, however, the $\epsilon$-expansion of the right-hand-side performed at a finite $\zeta$:

$$\eta=\frac{\rho^2}{4}\frac{\zeta\epsilon}{4(N+8)}\left[1+\frac{2(N+2)}{N+8}\frac{\epsilon}{\zeta}\right]. \tag{49}$$

If we now take the limit $\zeta\to 0$, the right-hand-side starts directly like $\epsilon^2$. Together with the lowest-order value 1 of $\rho^2/4$, we obtain correctly Eq. (46).

For consistency, the different two-loop results for $\eta$, once from Eqs. (44) and (45), and once $\eta=0$ from Eq. (48) should not be too far from each other. This can indeed be verified by plotting the curves $\eta=2-\gamma/\nu$ against a few values of $N$. The curves are all close to the $\eta=0$ axis for all $N$, approaching it for $N\to\infty$.

Also for higher-loop orders, $\eta$ could be obtained from the strong-coupling limit of $\gamma$ and $\nu$, or by taking a direct strong-coupling limit. Variational perturbation theory does not know which of these approaches should be better. Ultimately, if we know enough terms in the series expansion, the extrapolation to infinite order $L$ should certainly become insensitive to which function is resummed.

One may wonder if it is possible to set up a unique optimal function of the critical exponents from which to derive the strong-coupling limit. The answer to this question would improve the theory considerably.

Collecting the different results of this section, we have the $D=3$ results

$$\omega=\frac{1}{-1+2\sqrt{1+3(3N+14)/(N+8)^2}}, \tag{50}$$

$$\gamma=\frac{2N^3+63N^2+540N+1492}{(N+8)^2(N+20)}, \tag{51}$$

$$\nu=\frac{N^3+31N^2+262N+714}{(N+8)^2(N+19)}, \tag{52}$$

$$\eta_m=\frac{2(N+2)}{2N+21}\left[1+\frac{3(3N+14)}{(N+8)^2}\right], \tag{53}$$

$$\eta=\frac{2(N+2)}{N+20}\frac{(N+8)^2+3(3N+14)}{2(N+8)^3+5(N+8)^2+3(N+2)(3N+14)}, \tag{54}$$

$$u^*=\frac{1}{4(N+8)}+\frac{3}{4}\frac{3N+14}{(N+8)^3}, \tag{55}$$

where we also included the value of the renormalized coupling constant at the IR-fixed point. It is obtained from the one-loop series in $u$ of the expansion (14):

$$u=\bar{u}_B-\frac{4(N+8)}{\epsilon}\bar{u}_B^2. \tag{56}$$

We can restrict ourselves to one loop since it corresponds to a power $\bar{u}_B^2$. The two-loop calculation was, however, needed to get $\omega$ correctly, which itself enters Eq. (56). With the help of Eq. (23), we obtain

$$u^*=\frac{\rho^2}{4}\frac{\epsilon}{4(N+8)}=\frac{\epsilon}{4(N+8)}+\frac{3}{4}\frac{3N+14}{(N+8)^3}\epsilon^2. \tag{57}$$

Since only two critical exponents are independent [12,13], all other can be derived from Eqs. (50)–(54). These two-loop expressions are only a lowest approximation to the exact results. In the next section, we evaluate analytically the strong-coupling limit of the exponents at the three-loop level.

### D. Critical exponents from three-loop expansions

The three-loop calculations are algebraically more involved. Moreover, as far as the critical exponents are concerned (we will see later that this is not necessarily true for the amplitude functions) the optimum of the function (17) is not given by the vanishing of the first derivative, but by a turning point, i.e., by the vanishing of the second derivative. At the three-loop order, this implies that the parameter $r$ in Eq. (24) is zero, leading to the three-loop strong-coupling limit result (25). It is this feature that renders the calculation analytically manageable, involving only a cubic equation for the determination of $\rho$ (without $r=0$, we would have had to solve an eight-order equation). In order to obtain $\omega$ to three loop, we generalize Eq. (32) to the same order, and find

$$\begin{aligned}-1\equiv&\frac{d}{d\ln\bar{u}_B}\ln\frac{u}{\bar{u}_B}\\ =&\frac{-4(N+8)}{\epsilon}\bar{u}_B+16\left[\frac{(N+8)^2}{\epsilon^2}+\frac{3(3N+14)}{\epsilon}\right]\bar{u}_B^2\\ &-8\left[\frac{8(N+8)^3}{\epsilon^3}+\frac{60(N+8)(3N+14)}{\epsilon^2}\right.\\ &\left.+\frac{96\zeta(3)(5N+22)+33N^2+922N+2960}{\epsilon}\right]\bar{u}_B^3.\end{aligned} \tag{58}$$

From this we extract the coefficients $f_i(i=0,\ldots,3)$ of Eq. (24). The argument of the square root $r$ then turns out to be negative, and the equation to be solved is Eq. (25). This is true not only for $\epsilon=1$, but also for all $\epsilon\in[0,1]$. Since Eq. (25) is a cubic equation for $\rho$, there are three solutions, one of which is always negative, which we discard as unphysical, leaving us with two solutions. Only one of them is connected smoothly to the two-loop result. The purely algebraic form of the solution, generalization of the square root coming from solving Eq. (34), is somewhat too lengthy to be written down here. As a check, we have derived its epsilon expansion that reads

$$\rho_\epsilon = 2 + \frac{3(3N+14)}{(N+8)^2}\epsilon - \frac{96\zeta(3)(5N+22)(N+8)+33N^3+214N^2+1264N+2512}{4(N+8)^4}\epsilon^2 \tag{59}$$

and leads to the correct $\epsilon$-expansion for $\omega = \epsilon/(\rho - 1)$:

$$\omega_\epsilon = \epsilon - \frac{3(3N+14)}{(N+8)^2}\epsilon^2 + \frac{96\zeta(3)(5N+22)(N+8)+33N^3+538N^2+4288N+9568}{4(N+8)^4}\epsilon^3, \tag{60}$$

which is the extension of Eq. (36) to the order $\epsilon^3$. This is to be compared with Eq. (17.15) of the textbook [13].

The trigonometric representation is, however, compact enough to be written down here explicitly, at least for $\epsilon = 1$. Introducing an angle $\theta$ and two coefficients $a_0, b_0$ defined by

$$\begin{aligned}\theta = \arccos\Bigg( & \frac{[13\,776+4738N+N^2(8N+405)+96(5N+22)\zeta(3)]^2}{2[106+N(N+28)]\{(N+8)[13\,776+4738N+N^2(8N+405)+96(5N+22)\zeta(3)]\}^{3/2}} \\ & \times \frac{1}{[2\,209\,664+1\,040\,160N+162\,982N^2+9683N^3+184N^4+672(N+8)(5N+22)\zeta(3)]^{3/2}} \\ & \times\{67\,181\,166\,592+64\,001\,040\,384N+25\,893\,312\,000N^2+5\,641\,828\,480N^3+713\,027\,988N^4+54\,733\,044N^5 \\ & +2\,760\,157N^6+88\,332N^7+1440N^8-192(N+8)(5N+22)[4\,084\,864+1\,952\,480N+323\,706N^2+20\,021N^3 \\ & +514N^4]\zeta(3)+746\,496[(N+8)(5N+22)\zeta(3)]^2\}\Bigg),\end{aligned} \tag{61}$$

$$a_0 = \frac{1}{446\,336+213\,280N+35\,334N^2+2179N^3+56N^4-864(N+8)(5N+22)\zeta(3)} \tag{62}$$

$$\begin{aligned} b_0 = {} & 3\sqrt{(N+8)[13776+4738N+N^2(8N+405)+96(5N+22)\zeta(3)]} \\ & \times\sqrt{[2\,209\,664+1\,040\,160N+162\,982N^2+9683N^3+184N^4+672(N+8)(5N+22)\zeta(3)]},\end{aligned} \tag{63}$$

the relevant root of Eq. (25) can be written as

$$\rho = -\frac{1}{6} + \frac{256}{3}a_0[106+N(N+25)]^2 - a_0 b_0 \cos\left(\frac{-2\pi+\theta}{3}\right). \tag{64}$$

For the physically interesting cases $N = 0, \ldots, 4$, we obtain the values for $D = 3$ dimensions

| $N$ | 0 | 1 | 2 | 3 | 4 |
|---|---|---|---|---|---|
| $\rho$ | 2.41829 | 2.40384 | 2.38683 | 2.36910 | 2.35157 |
| $\omega$ | 0.705073 | 0.712332 | 0.721069 | 0.730405 | 0.73988 |
| $\omega$ (Ref. [13]) | 0.8035 | 0.7998 | 0.7948 | 0.7908 | |
| $\omega$ (Ref. [18]) | 0.812 | 0.799 | 0.789 | 0.782 | 0.774 |

where we also indicated the theoretical values given in Refs. [13,18].

Figure 1 illustrates the two- and three-loop critical exponents of the approach to scaling $\omega = \epsilon/(\rho - 1)$ as a function of $N$ calculated from Eqs. (34) and (64), respectively. For comparison, we also give the three-loop unresummed result (60), evaluated at $\epsilon = 1$ and the theoretical values given in Tables 1 and 3 of [18]. The latter are based on a five-loop analysis supplemented by a large loop order analysis.

Once $\omega$ is known to three loops, the other exponents and the strong-coupling limit $u^*$ of the renormalized coupling constant can be determined to the same order. To obtain $u^*$, the two-loop expansion of $u$ in powers of $\overline{u_B}$ is enough since it is of order $\mathcal{O}(\overline{u}_B^3)$. Recall that the three-loop expansion of $u(\overline{u_B})$ is needed only to calculate $\omega$. From Eq. (14) we identify $f_1, f_2, f_3$ and use Eq. (25) [since the argument of the corresponding $r$ in Eq. (24) is negative] to obtain the critical value

$$u^*=\frac{\epsilon(N+8)\rho(\rho+1)(2\rho-1)}{12[2(N+8)^2+3\epsilon(3N+14)]}-\frac{2\epsilon(N+8)^3(2\rho-1)^3}{27[2(N+8)^2+3\epsilon(3N+14)]^2} \tag{65}$$

with $\rho$ from Eq. (64). If we use instead the $\epsilon$-expansion of $\rho$ given in Eq. (59), we obtain

$$u^*=\frac{\epsilon}{4(N+8)}+\frac{3}{4}\frac{3N+14}{(N+8)^3}\epsilon^2+\frac{4544+1760N+110N^2-33N^3-96(N+8)(5N+22)\zeta(3)}{32(N+8)^5}\epsilon^3. \tag{66}$$

In the same way, we find the strong-coupling limit of the critical exponents $\gamma$ and $\nu$, as defined in Eqs. (40) and (41) together with Eqs. (30) and (31), the latter two exponents being obtained from the mass (15) and wave function (16) renormalization, respectively. The three-loop perturbative expansions are

$$\gamma=1+2(N+2)\bar{u}_B-4(N+2)\left[\frac{2(N+8)}{\epsilon}-(N-4)\right]\bar{u}_B^2+4(N+2)\left[\frac{8(N+8)^2}{\epsilon^2}-\frac{4(2N^2-N-106)}{\epsilon}+194+N(2N+17)\right]\bar{u}_B^3, \tag{67}$$

$$\nu=\frac{1}{2}+(N+2)\bar{u}_B-2(N+2)\left[\frac{2(N+8)}{\epsilon}-(N-3)\right]\bar{u}_B^2+4(N+2)\left[\frac{4(N+8)^2}{\epsilon^2}-\frac{2(2N^2+N-90)}{\epsilon}+95+N(N+9)\right]\bar{u}_B^3, \tag{68}$$

from which it is straightforward to identify the expansion coefficients $f_0,\dots,f_3$ that enter Eq. (25), to obtain

$$\gamma=1-\frac{\epsilon(N+2)[\epsilon(N-4)-2(N+8)]\rho(\rho+1)(2\rho-1)}{3[8(N+8)^2-4\epsilon(2N^2-N-106)+\epsilon^2(2N^2+17N+194)]}+\frac{8\epsilon(N+2)[\epsilon(N-4)-2(N+8)]^3(2\rho-1)^3}{27[8(N+8)^2-4\epsilon(2N^2-N-106)+\epsilon^2(2N^2+17N+194)]^2}, \tag{69}$$

$$\nu=\frac{1}{2}-\frac{\epsilon(N+2)[\epsilon(N-3)-2(N+8)]\rho(\rho+1)(2\rho-1)}{12[4(N+8)^2-2\epsilon(2N^2+N-90)+\epsilon^2(N^2+9N+95)]}+\frac{\epsilon(N+2)[\epsilon(N-3)-2(N+8)]^3(2\rho-1)^3}{27[4(N+8)^2-2\epsilon(2N^2+N-90)+\epsilon^2(N^2+9N+95)]^2}, \tag{70}$$

where $\rho$ for $\epsilon=1$ can be obtained from Eq. (64). The associated $\epsilon$-expansions can be obtained using Eq. (59). They read

$$\gamma=1+\frac{N+2}{2(N+8)}\epsilon+\frac{(N+2)(N^2+22N+52)}{4(N+8)^3}\epsilon^2+\frac{(N+2)[3104+2496N+664N^2+44N^3+N^4-48(N+8)(5N+22)\zeta(3)]}{8(N+8)^5}\epsilon^3, \tag{71}$$

$$\nu=\frac{1}{2}+\frac{N+2}{4(N+8)}\epsilon+\frac{(N+2)(N+3)(N+20)}{8(N+8)^3}\epsilon^2+\frac{(N+2)[8640+5904N+1412N^2+89N^3+2N^4-96(N+8)(5N+22)\zeta(3)]}{32(N+8)^5}\epsilon^3. \tag{72}$$

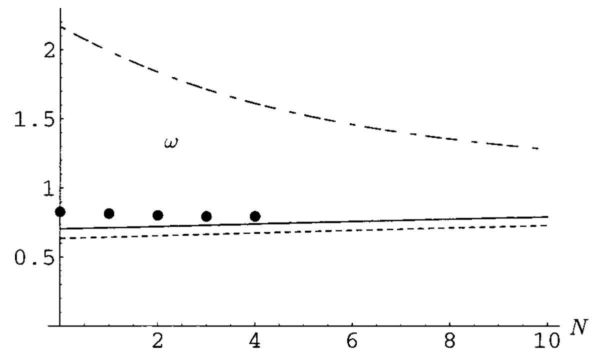


FIG. 1. Two-loop (short-dashed) and three-loop (solid) critical exponent $\omega$ for different O($N$) symmetries. For comparison, the $\epsilon$-expansion (mixed-dashed) and the theoretical values of [18] (dots) are also given.

Figures 2 and 3 illustrate the two- and three-loop critical exponents $\gamma$ and $\nu$, respectively, as a function of $N$. They are given by Eqs. (51) and (69) for $\gamma$ and by Eqs. (52) and (70) for $\nu$. For completeness, we also plot the $\epsilon$-expansions (71) and (72) of the exponents, as well as the theoretical values quoted in Tables 1 and 3 of [18]. Contrary to the case of the critical exponent $\omega$, we see that the two- and three-loop critical exponents are very close together. This is a virtue of working self-consistently with $\omega$ obtained at the same loop order. In [2,5], the extrapolated $\omega$ to infinite loop order was used instead. This implies that each loop-order result for $\gamma$ and $\nu$ was not very close to its asymptotic limit (contrary to what we get here). However, the extrapolation formula (19) works precisely for this case, and very precise extrapolated results for $\gamma$ and $\nu$ could be obtained. In our present work, the critical exponents are not very far from their asymptotic limit, already at the two- and three-loop level. However, the extrapolation formula (19) cannot be used. It is not yet clear to the authors how it will be possible to extrapolate the five-loop results obtained using the present formalism. This question is left aside for a future work. We also note in passing that the $\epsilon$-expansion result is not too far from the values obtained in the strong-coupling limit.

The critical exponent $\eta$ is obtained using $2-\gamma/\nu$, with $\gamma$ and $\nu$ from Eq. (69) and (70), respectively. It has the $\epsilon$ expansion

$$\eta=\frac{(N+2)}{2(N+8)^2}\epsilon^2-\frac{(N+2)(N^2-56N-272)}{8(N+8)^4}\epsilon^3. \quad (73)$$

Let us also calculate directly the strong coupling limit of $\eta$ from its definition (31):

$$\eta=8(N+2)\bar{u}_B^2-8(N+2)(N+8)\left(\frac{8}{\epsilon}+1\right)\bar{u}_B^3. \quad (74)$$

At the two-loop level, the result was zero. At the three-loop level, the calculation is different from that of $\gamma$ and $\nu$ because there is no linear term in $\bar{u}_B$. This has already been discussed after Eq. (26): although we are working at the three-loop level, the optimum of the variational perturbation theory is not governed by a turning point but by an extremum for which the sign of the root $r$ is the opposite to the usual case. The solution corresponds to $r=-1$ and the optimum is $\hat{u}_B=-2\bar{f}_2/(3f_3)$, so that

$$\eta=\frac{4}{27}\frac{\bar{f}_2^3}{f_3^2}=\frac{32}{27}\frac{(2\rho-1)^3(N+2)}{(N+8)^2(8+\epsilon)^2}\epsilon^2. \quad (75)$$

With Eq. (59), this leads again to the correct $\epsilon$-expansion (73). The difference between $\eta=2-\gamma/\nu$ and Eq. (75) at $\epsilon=1$ is illustrated in Fig. 4 that also shows the direct evaluation of the $\epsilon$-expansion series (73) as well as the theoretical values quoted in Tables 2 and 3 of [18].

It is amusing to see that the $\epsilon$ expansion is the best approximation, followed by the strong-coupling limit of the direct series (75). Comparing the different results, we see that they differ by about 30%. This is due to the absolute smallness of $\eta$. The error is small compared to unity.

To end this section we also give the critical exponent $\eta_m$. Up to three loops, the bare perturbation expansion reads, from Eqs. (15) and (30),

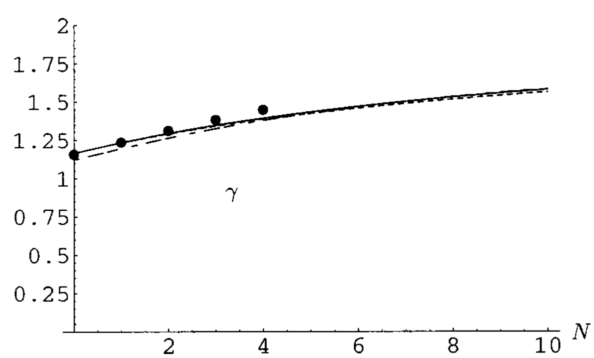


FIG. 2. Two-loop (short-dashed) and three-loop (solid) critical exponent $\gamma$. For comparison, the $\epsilon$-expansion (short- and long-dashed) and the theoretical values of [18] (dots) are also given.

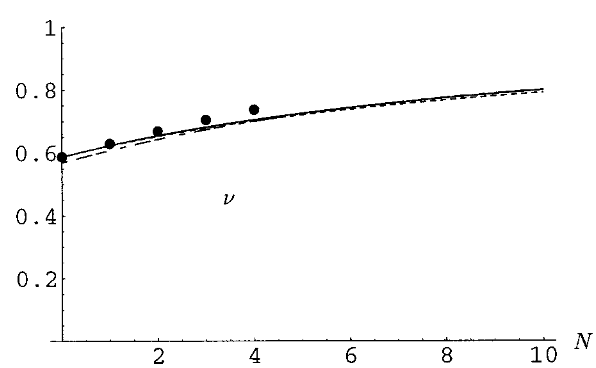


FIG. 3. Two-loop (short-dashed) and three-loop (solid) critical exponent $\nu$. For comparison, the $\epsilon$-expansion (short- and long-dashed) and the theoretical values of [18] (dots) are also given.

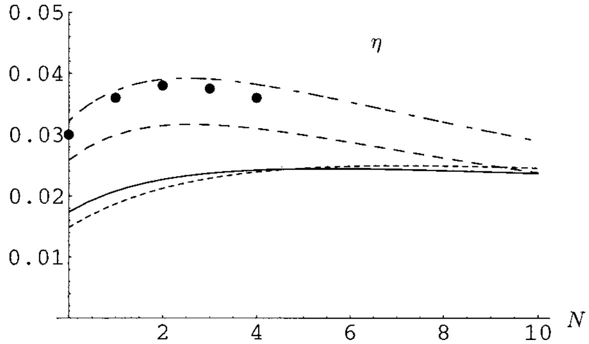


FIG. 4. Two-loop (short-dashed) and three-loop (solid) critical exponent $\eta$ from the definition $2-\gamma/\nu$. For comparison, the $\epsilon$ expansion (short- and long-dashed), $\eta$ from the strong-coupling limit of the direct (medium-dashed) series (75) and the theoretical values of [18] (dots) are also given.

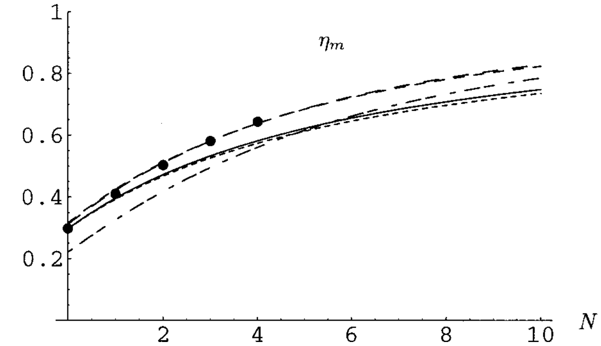


FIG. 5. Two-loop (short-dashed) and three-loop (solid) critical exponent $\eta_m$ from the definition $2-\nu^{-1}$. For comparison, the $\epsilon$ expansion (short- and long-dashed), $\eta_m$ from the strong-coupling limit of the direct (medium-dashed) two-loop (39) and three-loop (long-dashed) series (77) and the theoretical values of [18] (dots) are also given.

$$\eta_m=4(N+2)\overline{u}_B-8(N+2)\left[\frac{2(N+8)}{\epsilon}+5\right]\overline{u}_B^2+16(N+2)\times\left[\frac{4(N+8)^2}{\epsilon^2}+\frac{2(19N+122)}{\epsilon}+3(5N+37)\right]\overline{u}_B^3, \quad (76)$$

from which we deduce the strong-coupling limit with $\rho$ from Eq. (64)

$$\eta_m=\frac{\epsilon(N+2)(2N+16+5\epsilon)\rho(\rho+1)(2\rho-1)}{3[4(N+8)^2+\epsilon(38N+244)+3\epsilon^2(5N+37)]}-\frac{4\epsilon(N+2)(2N+16+5\epsilon)^3(2\rho-1)^3}{27[4(N+8)^2+\epsilon(38N+244)+3\epsilon^2(5N+37)]^2}. \quad (77)$$

Its $\epsilon$ expansion is

$$\eta_m=\frac{N+2}{N+8}\epsilon+\frac{(N+2)(13N+44)}{2(N+8)^3}\epsilon^2+\frac{(N+2)[5312+2672N+452N^2-3N^3-96(N+8)(5N+22)\zeta(3)]}{8(N+8)^5}\epsilon^3. \quad (78)$$

The result (77) is analytically different but numerically close to that obtained via the scaling relation (41), implying $\eta_m=2-\nu^{-1}$, as illustrated in Fig. 5. For completeness, the figure also shows the $\epsilon$ expansion (78) and the theoretical values quoted in Tables 2 and 3 of [18].

We see a better agreement with the theoretical values quoted from [18] when the exponent is evaluated in the strong-coupling limit of the direct series (39) and (77). This was also the same for the exponent $\eta$.

Collecting the different results of this section, we have the analytical form of the $D=3$ dimensions critical exponents in the three-loop order

$$\omega=\frac{1}{\rho-1}, \quad (79)$$

$$\gamma=1+\frac{(N+2)(N+20)\rho(\rho+1)(2\rho-1)}{3(2N^2+149N+1130)}-\frac{8(N+2)(N+20)^3(2\rho-1)^3}{27(2N^2+149N+1130)^2}, \quad (80)$$

$$\nu=\frac{1}{2}+\frac{(N+2)(N+19)\rho(\rho+1)(2\rho-1)}{12(N^2+71N+531)}-\frac{(N+2)(N+19)^3(2\rho-1)^3}{27(N^2+71N+531)^2}, \quad (81)$$

$$\eta_m=\frac{(N+2)(2N+21)\rho(\rho+1)(2\rho-1)}{3(4N^2+117N+611)}-\frac{4(N+2)(2N+21)^3(2\rho-1)^3}{27(4N^2+117N+611)^2}, \quad (82)$$

$$\eta=\frac{32}{2187}\frac{(2\rho-1)^3(N+2)}{(N+8)^2}, \quad (83)$$

$$u^*=\frac{(N+8)\rho(\rho+1)(2\rho-1)}{12[2(N+8)^2+3(3N+14)]}-\frac{2(N+8)^3(2\rho-1)^3}{27[2(N+8)^2+3(3N+14)]^2}, \quad (84)$$

where $\rho$ is given in Eq. (64). For $\eta$ and $\eta_m$, we took the strong-coupling limit of the direct expansions: Eq. (75) for $\eta$ and Eq. (77) for $\eta_m$. These results have to be compared with the two-loop ones given in Eqs. (50)–(54).

For completeness, we give below the table of the critical exponents to three loops and the comparison with Refs. [13,18]:

| $N$ | 0 | 1 | 2 | 3 | 4 |
|---|---|---|---|---|---|
| $\gamma$ | 1.16455 | 1.2338 | 1.29426 | 1.34697 | 1.39307 |
| $\gamma$ (Ref. [13]) | 1.1576 | 1.2349 | 1.3105 | 1.3830 | |
| $\gamma$ (Ref. [18]) | 1.1596 | 1.2396 | 1.3169 | 1.3895 | 1.456 |
| $\nu$ | 0.587376 | 0.623381 | 0.654552 | 0.681561 | 0.705071 |
| $\nu$ (Ref. [13]) | 0.5874 | 0.6292 | 0.6697 | 0.7081 | |
| $\nu$ (Ref. [18]) | 0.5882 | 0.6304 | 0.6703 | 0.7073 | 0.741 |
| $\eta_m$ | 0.311607 | 0.421796 | 0.509799 | 0.580684 | 0.638337 |
| $\eta_m$ (Ref. [13]) | 0.2976 | 0.4107 | 0.5068 | 0.5878 | |
| $\eta_m$ (Ref. [18]) | 0.2999 | 0.4137 | 0.5081 | 0.5862 | 0.6505 |
| $\eta$ | 0.0258218 | 0.029917 | 0.031452 | 0.0315846 | 0.03096 |
| $\eta$ (Ref. [13]) | 0.0316 | 0.0373 | 0.0396 | 0.0367 | |
| $\eta$ (Ref. [18]) | 0.0284 | 0.0335 | 0.0354 | 0.0355 | 0.0350 |

They cannot compete with the five-loop calculation of [2–6,13,18]. However, our results are analytical, and already close to the asymptotic limit although we made no assumption about the large-order behavior of the theory. We consider this as promising. In a subsequent publication, we will present a numerical calculation up to five loops, with large-order behavior information included, of our self-consistent formalism.

## IV. CALCULATION OF AMPLITUDE FUNCTIONS AND RATIOS

From now on, we shall focus entirely upon the $D=3$-dimensions model. As we mentioned in the introduction, it is only for the critical exponents that the minimal subtraction scheme leads to the same resummed values both for $D=3$ and $D=4-\epsilon$. For this reason, it made sense to study the $\epsilon$-expansions of the critical exponents, which was also useful for comparing with calculations in $4-\epsilon$ dimensions. The reason for this equality is the mass independence of the renormalization constants in this MS scheme. The mass independence implies a decomposition of the correlation functions into amplitude functions and power parts, for which the latter can be evaluated in the symmetric phase. The amplitude functions, however, depend on being in the ordered or disordered phase. Moreover, the situation is complicated for $N>1$ by the presence of Goldstone singularities, most of which have to be canceled at the end of the calculations: only the physical singularities, for example, those occurring in the transverse susceptibilities, should stay at the end of the calculations.

For this reason, apart from the three-loop work [41], no three- or higher-loop calculation has been done for $N>1$ below $T_c$, even numerically. The only relatively easy case is $N=1$ for which extensive numerical work has been done below $T_c$ up to five-loop order [21,25,40]. Above $T_c$, all $N$ can be treated in the same way [20,24,51]. In the latter reference the critical exponents $\eta$ and $\eta_m$ have even been obtained to seven loops, with resummation performed in [3,13,21,52].

We have explained in detail in the first part of this paper that it is unnecessary to go to the renormalized theory since all results can be obtained from the strong-coupling limit of the bare theory. In the literature, the effective potential is given in terms of the renormalized quantities [42,41,46]. To apply our theory, we shall rewrite the expressions back in the bare form, using Eq. (14).

### A. Available expansions

Let us list the most important available amplitude functions derived from the minimally renormalized model at $D=3$ at vanishing external magnetic field $h_B$. Up to two loops, they can be found in Ref. [46]: the square of the order parameter $M_B^2=\langle\phi_B^2\rangle$ below $T_c$:

$$f_\phi=\frac{1}{32\pi u}+\left[\frac{1}{27\pi}(160-82N)+\frac{2}{\pi}(N-1)\ln 3\right]u, \tag{85}$$

the stiffness of phase fluctuations below $T_c$ (some authors call this helicity modulus [53]) $\Upsilon$:

$$f_\Upsilon=\frac{1}{8u}+\frac{1}{3}+\left[\frac{1}{54}(2378-683N)+8(N-3)\ln 3\right]u, \tag{86}$$

the $q^2$ part of the transverse susceptibility $\chi_T$:

$$f_{\chi_T}=1+\frac{8}{3}u+\left[\frac{488}{3}-4N-128\ln 3\right]u^2, \tag{87}$$

the specific heat $C^\pm$ above and below $T_c$:

$$F_+=-N-2N(N+2)u, \tag{88}$$

$$F_-=\frac{1}{2u}-4+8(10-N)u, \tag{89}$$

the isotropic susceptibility above $T_c$ [55]

$$f_{\chi_+}=1-\frac{92}{27}(N+2)u^2, \tag{90}$$

the amplitude function of the susceptibility below $T_c$, which we obtain taking the inverse of the two loop numerical expansion given (up to five loops) in [40]:

$$f_{\chi_-}=1+18u+164.44u^2. \tag{91}$$

The latter quantity is restricted to $N=1$.

From the series expansion of $f_{\chi_T}$ and $f_\Upsilon$, one sees that the relation

$$f_\Upsilon=4\pi f_\phi f_{\chi_T} \tag{92}$$

is satisfied to two loops. This is not a surprise: the bare helicity modulus, defined as $\Upsilon=2\partial\Gamma_B/\partial q^2|_{q=0}$ where $\Gamma_B$ is the free energy, can be shown (at least to two loops [46]) to be identical to $M_B^2(\partial\chi_T^{-1}/\partial q^2)|_{q=0}$. This is a consequence of a Ward identity for the broken O($N$)-symmetry below $T_c$.

In Ref. [42], the perturbation expansions of the amplitude functions for the order parameter and for the specific heat have been carried to three loops. The additional terms are (we use the notation $f_j=\Sigma_i f_j^{(i)}u^i$):

$$\begin{aligned}f_\phi^{(3)}=&-\frac{1}{1080\pi}\Bigg\{2500N^2+65\,104N+29\,056+8640(5N\\&+22)\zeta(3)+58\,320c_1-15\pi^2(19N^2+643N+499)\\&-180(64N^2+640N+457)\mathrm{Li}_2\left(-\frac{1}{3}\right)-80(194N^2\\&+1616N-1675)\ln 3+16(860N^2+8357N-7867)\ln 2\\&+270(N-1)\Bigg[-8c_2+32\mathrm{Li}_2\left(-\frac{1}{2}\right)+42\mathrm{Li}_2\left(\frac{1}{3}\right)\\&-64\mathrm{Li}_2(-2)+21(\ln 3)^2+16(\ln 2)^2-96(\ln 2)\\&\times(\ln 3)\Bigg]\Bigg\},\end{aligned} \tag{93}$$

$$F_+^{(3)}=-4N(N+2)\left(N-\frac{7}{27}+4\ln\frac{4}{3}\right), \tag{94}$$

$$\begin{aligned}F_-^{(3)}=&-\frac{1}{27}(1080N^2+3464N+31120)-128(5N+22)\zeta(3)\\&-864c_1+\frac{2}{3}\pi^2(9N^2+N+17)+216\mathrm{Li}_2\left(-\frac{1}{3}\right)\\&-32(4N+17)\ln 3+\frac{32}{3}(31N+95)\ln 2\\&+4(N-1)\Bigg[-8c_2+16\mathrm{Li}_2\left(-\frac{1}{2}\right)\\&+6\mathrm{Li}_2\left(\frac{1}{3}\right)-32\mathrm{Li}_2(-2)+3(\ln 3)^2+8(\ln 2)^2\\&-48(\ln 2)(\ln 3)\Bigg],\end{aligned} \tag{95}$$

where $\mathrm{Li}_2(x)=\Sigma_{n=0}^\infty x^n/n^2$ is the dilogarithmic function [54], and $c_1$ and $c_2$ are two numerical constants given by a single variable integration over elementary functions [35,42]:

$$\begin{aligned}c_1=&\int_0^1\frac{dx}{\sqrt{6-2x^2}}\left[\ln\frac{3}{4}+\ln\frac{3+x}{2+x}+\frac{x}{2+x}\right.\\&\left.\times\left(\ln\frac{3+x}{3}+\frac{x}{2-x}\ln\frac{2+x}{4}\right)\right]\\&\approx 0.021\,737\,576\,333,\end{aligned} \tag{96}$$

$$\begin{aligned}c_2=&\frac{\pi^2}{4\sqrt{2}}+\sqrt{2}\int_0^1\frac{dx}{\sqrt{1+x^2}}\left[\ln\frac{x}{1+x}+\frac{\ln(1+x)}{x}\right]\\&\approx 0.973\,771\,427.\end{aligned} \tag{97}$$

For completeness, we give in Appendix B some hints on how to obtain these amplitude functions. For the details, see Refs. [41,46]. Our own contribution concerns the susceptibilities above and below $T_c$: Using the three-loop integrals available in the literature [42,35], we have been able to calculate analytically the thee-loop extension of the amplitude of the isotropic susceptibility $f_{\chi_+}$:

$$\begin{aligned}f_{\chi_+}^{(3)}=&-\frac{8}{27}(N+2)(N+8)\\&\times\left[-21+12\pi^2+128\ln\frac{3}{4}+144\mathrm{Li}_2\left(-\frac{1}{3}\right)\right],\end{aligned} \tag{98}$$

as well as the three-loop amplitude function of the susceptibility below $T_c$, for $N=1$:

$$\begin{aligned}f_{\chi_-}=&1+18u+\frac{1480}{9}u^2+\left[1072-11\,664c_1+3\pi^2\right.\\&\left.+10\,480\ln\frac{4}{3}+36\mathrm{Li}_2\left(-\frac{1}{3}\right)\right]u^3.\end{aligned} \tag{99}$$

Our analytical two-loop coefficient 1480/9 agrees with the numerical coefficient given in Eq. (91). We shall comment on the three-loop one later. The details of the calculation are given in Appendixes C and D.

### B. Amplitude ratios

Besides the amplitude functions, we shall also evaluate three important ratios: the amplitude ratio of the heat capacity, the universal combination $R_C$, and the amplitude ratio of the susceptibilities for $N=1$. For a review of amplitude ratios, see [56]. The relevant equations for their determination is given in Appendix E. One of the best measured amplitude ratios was mentioned in the introduction: it is the amplitude ratio of the specific heat of superfluid helium above and below $T_c$, corresponding to $N=2$. It can, however, be defined for all $N$ and, using our notation, can be written as [38,42]

$$\frac{A^+}{A^-}=\left(\frac{b^+}{b^-}\right)^{\alpha}\left(\frac{4\nu B^*+\alpha F_+^*}{4\nu B^*+\alpha F_-^*}\right), \tag{100}$$

where $\alpha$ and $\nu$ are critical exponents and $B^*$ is the vacuum renormalization group function associated with the additive renormalization constant of the vacuum, evaluated at the critical point. It is known to five loops in the minimal subtraction scheme [42,43] and reads, up to three loops,

$$uB=\frac{N}{2}u+3N(N+2)u^3. \tag{101}$$

The ratio $b^+/b^-$ is equal to [41]: $b^+/b^-=2\nu P_+^*/[(3/2)-2\nu P_+^*]$, where $P_+$ is a polynomial in $u$, related to the scale above $T_c$. Its analytical derivation is given in Appendix F and reads, up to three loops,

$$P_+=1-2(N+2)u+4(N+2)u^2+\frac{8}{27}(N+2)\times\left[-3(63N+572)+24(N+8)\pi^2+4(43N+182)\ln\frac{3}{4}+288(N+8)\mathrm{Li}_2\left(-\frac{1}{3}\right)\right]u^3. \tag{102}$$

The experimental test for the validity of the strong-coupling expansion is to match Eq. (100) with (1) for $N=2$. We shall see in the next subsection if this can be done.

The ratio $R_C$ is defined by the universal combination of amplitudes [56] $R_C=\Gamma^+A^+/A_M^2$ where $\Gamma^+$ and $A_M$ are the leading amplitudes of the isotropic susceptibility above $T_c$ and of the order parameter below $T_c$, respectively. This ratio has been written in Ref. [42] as

$$R_C=\frac{(2\nu P_+^*)^{2-2\beta}}{(3/2-2\nu P_+^*)^{-2\beta}}\,\frac{4\nu B^*+\alpha F_+^*}{16\pi}\,\frac{1}{f_\phi^* f_{\chi_+}^*}. \tag{103}$$

All the quantities have been defined previously, but for $\beta$ which may be taken from the hyperscaling relation $\beta=\nu(D-2+\eta)/2=\nu(1+\eta)/2$ in $D=3$ dimensions. However, our own calculation for $R_C$ gives a correction to Eq. (103):

$$R_C=\frac{(2\nu P_+^*)^{2-\nu(D-2)}}{(3/2-2\nu P_+^*)^{-\nu(D-2)}}\,\frac{4\nu B^*+\alpha F_+^*}{16\pi}\,\frac{1}{f_\phi^* f_{\chi_+}^*}=\frac{(2\nu P_+^*)^{2-2\beta}}{(3/2-2\nu P_+^*)^{-2\beta}}\left(\frac{b^+}{b^-}\right)^{\nu\eta}\frac{4\nu B^*+\alpha F_+^*}{16\pi}\,\frac{1}{f_\phi^* f_{\chi_+}^*}. \tag{104}$$

Since this disagrees with Eq. (103), we give our derivation of this result in Appendix E. We have verified that the numerical values coming from Eqs. (103) and (104) do agree within 1%. This is traced back to the small value of the exponent $\eta$.

In the following we shall, however, consider Eq. (104). We hope than the analytical discrepancy between Eq. (103) and (104) will soon be resolved.

The third ratio to be investigated is the amplitude ratio of the susceptibilities for $N=1$. Such a ratio can also be defined for the longitudinal susceptibilities for $N>1$. This is a nontrivial task requiring an appropriate description [57] due to Goldstone singularities and this will not be investigated here. Using the notation of [40,55], the amplitude ratio can be written as

$$\frac{\Gamma^+}{\Gamma^-}=\frac{f_{\chi_-}^*}{f_{\chi_+}^*}\left(\frac{\xi_+}{\xi_-}\right)^2=\frac{f_{\chi_-}^*}{f_{\chi_+}^*}\left(\frac{b^+}{b^-}\right)^{2\nu}, \tag{105}$$

where the ratio $b^+/b^-$ has been defined below Eq. (100), and where the quantities are restricted to $N=1$.

The question arises now to calculate the amplitude functions and ratios. As for the case of the critical exponents, we shall proceed also by order, starting with two loops.

### C. Amplitude functions from two-loop expansions

In order to apply strong-coupling theory to the amplitude functions (85)–(88), we must reexpand them in powers of the bare coupling $\overline{u_B}$ using Eq. (14) up to two loops. The strong-coupling limit is then given by the general expression (23), with $\rho^2/4$ given by Eq. (34) at $\epsilon=1$.

We start considering $f_\phi$. To deal with a Taylor series, as assumed in the general theory in Sec. III A, we consider $uf_\phi$:

$$uf_\phi=\frac{1}{32\pi}+\left[\frac{1}{27\pi}(160-82N)+\frac{2}{\pi}(N-1)\ln 3\right]\overline{u}_B^2. \tag{106}$$

This series is special because the linear term in $\overline{u_B}$, is absent: the optimal value (23) is therefore given by $\hat{u}_B^*=0$, and the two-loop value of $uf_\phi$ in the strong-coupling limit is the same as the lowest-order value, which is independent of $N$:

$$u^*f_\phi^*=\frac{1}{32\pi}. \tag{107}$$

It is worth pointing out here the effect of the special choice for $A_D$ in Eq. (8). We mentioned there that this coefficient did not have any influence upon the critical exponent. This is because the factor $A_D$ can be absorbed in $u_B$ to give $\overline{u_B}$, implying the same strong-coupling limit. However, amplitude functions are $A_D$ dependent. In particular, for $uf_\phi$, the chosen value $A_3=1/(4\pi)$ has made the linear term disappear. One sees that this choice corresponds to an optimalization: the zero order, the one-loop and the two-loop optimum values coincide. One expects then that the third-loop order contributes only to a small deviation from it. This is indeed the case, as will be shown in the next section, and confirm previous expectations [38,41].

The same situation holds for the amplitude function (90) of the susceptibility above $T_c$. The linear term in $u$ being absent, the optimal value to two loops is independent of $N$ and is equal to

$$f^*_{\chi_+}=1. \tag{108}$$

The strong-coupling limit of the amplitude function of the stiffness of phase fluctuations and of the $q^2$-dependent part of the transverse susceptibility can also be easily determined. The bare expansion is obtained combining Eqs. (86), (87), and (14) to two loops:

$$uf_\Upsilon=\frac{1}{8}+\frac{\bar{u}_B}{3}+\left[\frac{1}{54}(1802-755N)+8(N-3)\ln 3\right]\bar{u}_B^2, \tag{109}$$

$$f_{\chi_T}=1+\frac{8}{3}\bar{u}_B-\frac{4}{3}(11N-58+96\ln 3)\bar{u}_B^2. \tag{110}$$

The corresponding optima are given by Eq. (23) with Eq. (34) from which we obtain

$$u^*f^*_\Upsilon=\frac{1}{8}+\frac{6(N^2+25N+106)}{(N+8)^2[755N-1802-(432N-1296)\ln 3]}, \tag{111}$$

$$f^*_{\chi_T}=1+\frac{16(N^2+25N+106)}{3(N+8)^2[11N-58+96\ln 3]}. \tag{112}$$

The result (111) has a pole for $N=2(648\ln 3-901)/(432\ln 3-755)\approx 1.349$, indicating that the strong-coupling result is unreliable. We expect the pole to be an artifact of the limitation to two that disappears at the three-loop level. Since $f_\Upsilon$ is not known to three-loops, we can only give plausible arguments for this expectation, suggested by the calculation of $u^*(F^*_- - F^*_+)$ up to three loops in Eq. (136), where a similar pole arises at the two-loop level but disappears for three loops due to the interplay of the coefficients of the loop expansion. The trouble with Eq. (111) derives from the fact that the term of order $\bar{u}_B^2$ in Eq. (109) changes sign for the mentioned value of $N\approx 1.349$, and at the two-loop level nothing can compensate this. This is in contrast with critical exponents that were observed to be alternating series in powers of $\bar{u}_B$. The result (112) for $f_{\chi_T}$ is smooth for all positive $N$. A more reliable result for $f^*_\Upsilon$ than the singular Eq. (111) can therefore be obtained by combining Eq. (107) with Eq. (112) via relation (92), leading to

$$f^*_\Upsilon=f^*_{\chi_T}/8. \tag{113}$$

Note that for $N\geqslant 4$, far away from the pole, the two results (111) and (113) agree within 2%.

It is worth pointing out that an evaluation of the renormalized expression (87) at the critical point $u^*$ given by eq. (55) leads to a result compatible with Eq. (112) within less that 1%. This is due to the fact that higher-order correction to the zero-order result $f_{\chi_T}=1$ are small for all $N$. This is in contrast to $f_\phi$ and $f_\Upsilon$, where two-loop corrections are important.

We now turn to the amplitude functions $F_\pm$ that enter the heat capacity above and below $T_c$. At the two-loop level, they are given by Eqs. (88) and (89), respectively. With the relation between the renormalized and bare coupling constant (14) to two loops, we have the expansions

$$uF_+=-N\bar{u}_B+2N(N+14)\bar{u}_B^2, \tag{114}$$

$$uF_-=\frac{1}{2}-4\bar{u}_B+8(N+26)\bar{u}_B^2. \tag{115}$$

With the help of Eqs. (23) and (34), we obtain

$$u^*F^*_+=-\frac{N}{2}\frac{N^2+25N+106}{(N+8)^2(N+14)}, \tag{116}$$

$$u^*F^*_-=\frac{1}{2}-2\frac{N^2+25N+106}{(N+8)^2(N+26)}. \tag{117}$$

In [41,42], $uF_+$ was not a good candidate for Borel resummation because its $u$ expansion (88) lacks alternating signs of its coefficients. This problem is absent in variational perturbation theory since the expansion (114) in term of the bare coupling constant $\bar{u}_B$ does have alternating sign. The latter is then expected to lead to a reliable result (116). This will be confirmed by the three-loop result of the next section.

To apply the usual Borel resummation at the level of the renormalized quantities, Refs. [41,42] wrote the amplitude ratio of the heat capacity as

$$\frac{A^+}{A^-}=\left(\frac{b^+}{b^-}\right)^\alpha\left(1-\alpha\frac{F^*_- - F^*_+}{4\nu B^*+\alpha F^*_-}\right), \tag{118}$$

instead of Eq. (100), and resummed $u(F_- - F_+)$ and $uF_-$, avoiding the direct resummation of $uF_+$. For comparison, we give below the optimal value of the difference $u(F_- - F_+)$. It is determined from the expansions (88) and (89). Using Eq. (14), it yields

$$u(F_- - F_+)=\frac{1}{2}+(N-4)\bar{u}_B-2(N^2+10N-104)\bar{u}_B^2. \tag{119}$$

Its strong-coupling limit is, from Eqs. (23) and (34):

$$u^*(F^*_- - F^*_+)=\frac{1}{2}+\frac{(N-4)^2(N^2+25N+106)}{2(N+8)^2(N^2+10N-104)}. \tag{120}$$

The latter expression diverges for a positive value of $N=-5+\sqrt{129}\approx 6.358$. Then, the difference $u(F_+ - F_-)$ is not the good quantity for the strong-coupling limit at the two-loop level. We should rather evaluate $uF_+$ and $uF_-$ separately in the amplitude ratio (100), instead of using the equivalent expression (118). We shall see in the next section

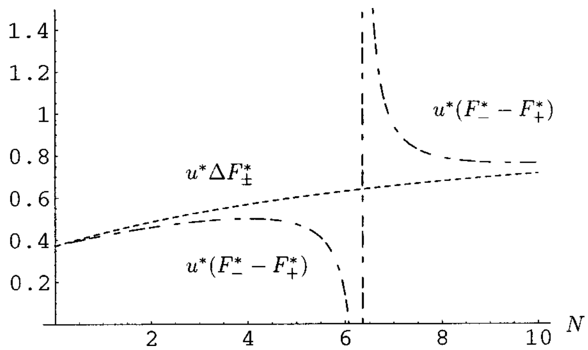


FIG. 6. Comparison between the two-loop strong-coupling limit of $u^*(F_-^* - F_+^*)$ and $u^*\Delta F_\pm^*$.

that the pole of $u^*(F_+^* - F_-^*)$ is an artifact of the two-loop calculation. A similar conclusion was also obtained for the strong-coupling limit of $f_{\Upsilon}$, see Eqs. (111) and (113). For $N \ll 4$ and for $N \gg -5 + \sqrt{129}$, the two-loop expansion (119) is alternating, and we expect that the strong-coupling result (120) is reliable. As an indication for this, we compare Eq. (120) with the difference of the optimized $u^*F_\pm^*$ values given in Eqs. (116) and (117):

$$u^*\Delta F_\pm^* = \frac{1}{2} - \frac{N^2+25N+106}{(N+8)^2}\left(\frac{2}{N+26} - \frac{N}{2(N+14)}\right). \tag{121}$$

In Fig. 6, we compare the two curves (120) and (121).

As far as the amplitude ratio of the heat capacity (100), or Eq. (118), is concerned, we still need to determine the strong-coupling limit of the renormalization group function $B(u)$ of the vacuum (101) and of the polynomial $P_+$ defined in Eq. (102). Because there is no contribution of the two-loop order to Eq. (101), its strong-coupling limit is

$$u^*B^* = u^*\frac{N}{2}. \tag{122}$$

Since the optimal two-loop result is identical to the one-loop result, it is clear that we may expect the large order limit $L \to \infty$ to differ only little from $N/2$. This has been confirmed in the five-loop resummation performed in [41], and will be also seen in our three-loop calculation in the next section.

The polynomial $P_+$ given in Eq. (102) is evaluated in the strong-coupling limit using the same lines. The starting point is the expansion in powers of the bare coupling constant given in Eq. (F4) of Appendix F. Its two-loop part combined with Eqs. (23) and (34) leads to

$$P_+^* = 1 - \frac{(N+2)(N^2+25N+106)}{(N+8)^2(2N+17)}. \tag{123}$$

The last amplitude we shall calculate using strong-coupling theory is $f_{\chi_-}$. From Eqs. (23) and (34) at $N=1$, and from the two-loop part of Eq. (D3), we find, with Eqs. (23) and (34),

$$f_{\chi_-}^* = 1 + 9\frac{\rho^2}{4}\,\frac{18^2}{4532} = 211/103. \tag{124}$$

Combining with the unit value (108) of $f_{\chi_+}^*$, we have a ratio $f_{\chi_-^*}/f_{\chi_+^*}$ identical to Eq. (124). However, this ratio might as well be determined as the strong-coupling limit of its perturbative expansion, instead of evaluating independently the strong-coupling limit of the numerator and the denominator. The relevant equation is given in Appendix D: Using the two-loop expansion of Eq. (D6), we have, with Eqs. (23) and (34),

$$\left(\frac{f_{\chi_-}}{f_{\chi_+}}\right)^* = 1 + \frac{\rho^2}{4}\,\frac{3\times 18^2}{1420} = \frac{751}{355}. \tag{125}$$

### D. Amplitude functions from three-loop expansions

Some of the amplitude functions have been obtained up to the three-loop order. We now turn to their strong-coupling limit. This is done by applying Eqs. (24), (25), and (64) to the different amplitude expansions.

We start with the amplitude function of the square of the order parameter. Combining the two-loop expansion (85) with the three-loop term $f_\phi^{(3)}$ (93), and using also the relation between the bare and renormalized coupling constant (14), we have the three-loop expansion

$$u f_\phi = \frac{1}{32\pi} + \left[\frac{1}{27\pi}(160-82N) + \frac{2}{\pi}(N-1)\ln 3\right]\bar{u}_B^2 + \left\{ f_\phi^{(3)} - 8(N+8)\left[\frac{1}{27\pi}(160-82N) + \frac{2}{\pi}(N-1)\ln 3\right]\right\}\bar{u}_B^3. \tag{126}$$

From this, we read off the expansion coefficients $f_0, f_1, f_2, f_3$ entering Eqs. (24), (25), and (64). Since the linear term $f_1$ vanishes, we have to follow the development below Eq. (26), adapting it to the present case. This development was done assuming a series with alternating sign since the expansions of the critical exponents had this property. Here, this is no longer true. Consider once more the derivation of the strong-coupling limit following from the optimal value of $f = f_0 + \overline{f_2}\hat{u}_B^2 + f_3\hat{u}_B^3$: $\hat{u}_B^*(2\overline{f_2} + 3f_3\hat{u}_B^*) = 0$. Two solutions are possible: $\hat{u}_B^* = 0$ and $\hat{u}_B^* = -2\overline{f_2}/(3f_3)$. The latter was relevant for the critical exponent $\eta$. This does not mean that the other solution has to be rejected. In fact, looking at the nature of the extremum (minimum or maximum), we see directly that the first solution corresponds to

$$\left.\frac{\partial^2 f}{\partial \hat{u}_B^2}\right|_{\hat{u}_B = \hat{u}_B^* = 0} = 2\overline{f_2}, \tag{127}$$

while the other leads to

$$\left.\frac{\partial^2 f}{\partial \hat{u}_B^2}\right|_{\hat{u}_B = \hat{u}_B^* = -2\overline{f_2}/(3f_3)} = -2\overline{f_2}. \tag{128}$$

If one solution is a maximum, the other one is a minimum. Looking for the sign of $\overline{f_2}$ in Eq. (126), we see that it is positive for $N<N_\phi$, with $N_\phi=(80-27\ln 3)/(41-27\ln 3)\approx 4.439\,92$, corresponding to a maximum, and negative for $N$ greater, corresponding to a minimum. Variational perturbation theory at loop order $L>1$ says nothing about the nature of the extremum. It might be a minimum or a maximum. In quantum mechanics, this has been explained in the book [1]. In quantum field theory, the exponent $\eta$ illustrates this: we had chosen the maximum [recall Eq. (75)]. In this way, the $\epsilon$-expansion was obtained. Taking the solution $\hat{u}_B^*=0$, corresponding to the minimum, we would have obtained the three-loop result $\eta=0$. The lack of reproducing the $\epsilon$-expansion gives a hint that the maximum solution has to be chosen. In the case of $f_\phi$ we can also argue that the maximum solution has to be chosen, although here there is no $\epsilon$-expansion available, by definition of the model. However, at the point where $f_3=0$, we have to recover an optimization problem of a quadratic equation in $\hat{u}_B$, see Eq. (126). We know for this function that, because no linear term is present, the strong-coupling limit is $u^*f_\phi=1/(32\pi)$. This implies that $\hat{u}_B^*=0$ at this point, i.e., that the maximum solution has to be chosen. By continuity, this remains true in a neighborhood. The nature of the solution can only be changed when both solutions are equal, i.e., for $N$ smaller than its value $N_\phi$ making $f_2$ vanish. Below $N_\phi$, we can imagine that we have an interchange of solutions, and that the minimum has to be chosen. In this case, we would have $u^*f_\phi^*=1/(32\pi)$ for all $N$. If we decide to keep the maximum for all $N$, which we could prove to be true only for $N\geqslant N_\phi$, this would imply that $\hat{u}_B^*=-2\overline{f_2}/(3f_3)$ has to be chosen below $N_\phi$ and $\hat{u}_B^*=0$ above. Below $N_\phi$ we have $f^*=f_0+4\overline{f_2^3}/(27f_3^2)$, as was the case for the critical exponent $\eta$, while above $N_\phi$, the solution is $f^*=f_0$. The strong-coupling limit of $f_\phi$ to three loops is then

$$u^*f_\phi^*=\frac{1}{32\pi}+\frac{4}{27}(2\rho-1)^3\frac{[(160-82N)/(27\pi)+2(N-1)(\ln 3)/\pi]^3}{\{f_\phi^{(3)}-8(N+8)[(160-82N)/(27\pi)+2(N-1)(\ln 3)/\pi]\}^2}\Theta\left(\frac{80-27\ln 3}{41-27\ln 3}-N\right) \tag{129}$$

with $\rho$ given by Eq. (64), and where $\Theta(x)$ is the step function of Heaviside, being equal to 1 for $x>0$ and being vanishing for $x<0$. As mentioned, we cannot be assured that for $N<N_\phi$ the maximum has still to be chosen. The possibility that the three-loop result is identical to the two-loop result remains. Would the above analysis not be performed, i.e., choosing the minimum solution everywhere, we would have obtained Eq. (129) without the step function, meaning the presence of a pole at the vanishing of the coefficient of the cubic term in Eq. (126), i.e., for $N\approx 4.929\,15$. We have checked that the solution is sharply peaked near this value so that it would appear that the optimal value is valid almost everywhere. In fact, since the pole gives a very peaked contribution, a calculation at fixed integer value of $N$ would have missed it completely, making one to believe that the resummation was correct. But this would not be true, the true solution being Eq. (129) everywhere. We give in Fig. 7 the comparison between our two- and three-loop results. Our values for $N<N_\phi$ lie above the two-loop result $1/(32\pi)$ obtained in Eq. (107). This is also the case for the resummed values given in [42] for $N=2,3$ as can be seen in the following:

| $N$ | 0 | 1 | 2 | 3 | 4 | $N>N_\phi=(80-27\ln 3)/(41-27\ln 3)$ |
|---|---|---|---|---|---|---|
| $u^*f_\phi^*$ (2 loops) | $1/(32\pi)$ | $1/(32\pi)$ | $1/(32\pi)$ | $1/(32\pi)$ | $1/(32\pi)$ | $1/(32\pi)=0.00994718$ |
| $u^*f_\phi^*$ (3 loops) | 0.0105523 | 0.0102518 | 0.0100884 | 0.00999735 | 0.00995195 | $1/(32\pi)$ |
| $u^*f_\phi^*$ (Ref. [42]) | | | 0.010099 | 0.00997 | | |

The agreement between our two- and three-loop order, and between our work and [42], is excellent. It is due to the fact that the term of order zero contains almost all information on this amplitude.

The three-loop amplitude functions $uF_+$ and $uF_-$ are given by Eqs. (88), (94), (89), and (95). As in the case of the previous amplitudes, the present expansions may not be alternating. This may make the argument of the parameter $r$ in Eq. (24) positive, so that Eq. (24) has to be used to obtain the strong-coupling limit rather than Eq. (25). However, Eq. (25) remains correct for all $N$ for $uF_+$, while the alternating property is lost for $uF_-$ for $N\gtrsim 40$. Since the physical cases correspond to $N=0,1,2,3,4$, we can ignore the alternative Eq. (24) and Eq. (25) is used throughout. Using the relation (14) between the bare and renormalized coupling constant, the three-loop bare extension of Eqs. (114) and (115) are

$$uF_+=-N\overline{u}_B+2N(N+14)\overline{u}_B^2+[F_+^{(3)}-24N(7N+46)]\overline{u}_B^3, \tag{130}$$

$$uF_-=\frac{1}{2}-4\overline{u}_B+8(N+26)\overline{u}_B^2+[F_-^{(3)}-480(3N+22)]\overline{u}_B^3. \tag{131}$$

This allows to identify the appropriate $f_0,f_1,f_2,f_3$ functions to enter Eq. (25). In the strong-coupling limit, we obtain

$$u^*F_+^* = \frac{2N^2(N+14)\rho(\rho+1)(2\rho-1)}{6[F_+^{(3)}-24N(7N+46)]} + \frac{2[2N(N+14)]^3(2\rho-1)^3}{27[F_+^{(3)}-24N(7N+46)]^2}, \tag{132}$$

$$u^*F_-^* = \frac{1}{2} + \frac{32(N+26)\rho(\rho+1)(2\rho-1)}{6[F_-^{(3)}-480(3N+22)]} + \frac{2[8(N+26)]^3(2\rho-1)^3}{27[F_-^{(3)}-480(3N+22)]^2}, \tag{133}$$

with $\rho$ from Eq. (64).

Figures 8 and 9 show the comparison between the two-loop results [(116) and (117)] of the previous section and the corresponding three-loop results [(132) and (133)], as well as a comparison with values given in [41], when available.

To be more precise concerning the comparison with [41], we give the appropriate values of $u^*F_-^*$:

| $N$ | 0 | 1 | 2 | 3 | 4 |
|---|---|---|---|---|---|
| $u^*F_-^*$ (2 loops) | 0.372596 | 0.379287 | 0.385714 | 0.391707 | 0.397222 |
| $u^*F_-^*$ (3 loops) | 0.374166 | 0.378474 | 0.384065 | 0.389883 | 0.395484 |
| $u^*F_-^*$ (Ref. [41]) | | 0.3687 | 0.384 | 0.387 | |

From this, we see that that the strong-coupling limit results for $u^*F_-^+$ at the three-loop level differ only a little from their two-loop counterpart. This was also see in Fig. 9 and Fig. 8 for $u^*F_+^*$. For $N=1$, we can also infer from the table that the results coming from variational perturbation theory and from a Borel resummation [41] are not in excellent agreement, not even within the error-bars of the latter: $u^*F_-^*(N=1)=0.3687\pm0.0040$. The agreement is, however, recovered for the values $N=2,3$.

For $u^*F_+^*$, there is no available comparison between our work and others. The authors of [41] could not perform a reliable Borel resummation, presumably because of the lack of an alternating series. A comparison is, however, possible for the difference $u^*(F_-^*-F_+^*)$. We have seen in the previous section that the two-loop evaluation of this difference in the strong-coupling limit did not work well in our case because the second-order term in the bare expansion changes sign for some value of $N$. Let us see how the situation changes at the three-loop level, which has the expansion [see Eqs. (130) and (131)]

$$u(F_- - F_+) = \frac{1}{2} + (N-4)\overline{u}_B - 2(N^2+10N-104)\overline{u}_B^2 + [F_-^{(3)} - F_+^{(3)} + 24(7N^2-14N-440)]\overline{u}_B^3. \tag{134}$$

The coefficient of the second-order term vanishes for $N=-5+\sqrt{129}$. This is not anymore a problem since there is a three-loop order term preventing a $1/f_2$ behavior, see the comparison between Eqs. (23) and (25). The coefficient of the three-loop order can itself vanish. For Eq. (134), this happens for $N\equiv\overline{N}\approx10.5324$. Since Eqs. (24) and (25) imply a behavior like $1/f_3$, it is legitimate to wonder about poles. The answer is simple: if the coefficient of the three-loop term vanishes, then the problem is formally equivalent to evaluating the strong-coupling limit of a two-loop series. The coefficient of the linear and quadratic terms are, however, different from the two-loop result since the linear term has a factor $\rho(\rho+1)/2$ instead of $\rho$ and the quadratic one a coefficient $(2\rho-1)$ instead of a factor 1. We conclude that when the three-loop term vanishes, the strong-coupling limit should be well behaved, giving a smooth curve around $\overline{N}$. This discussion shows that the function $r$ in Eq. (24) is not always zero here because $r$ contains the coefficient $f_2$ of the two-loop term, and its zero governs the behavior of the solution (24). We note here the important following point: the positive square root $+r$ was chosen in Eq. (24) in order to match a vanishing $f_3$. We explained, and this was used when evaluating $\eta$, that the negative root might play a role as well. For $\eta$ to three-loop order, we had a negative $r$. Let us see what happens for $f_2=0$. The expansion to be optimized is $f=f_0+\overline{f}_1\hat{u}_B+f_3\hat{u}_B^3$, such that we have to solve $\overline{f}_1+3f_3(\hat{u}_B^*)^2$

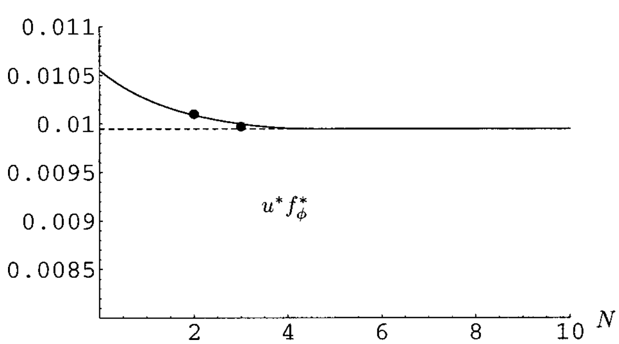


FIG. 7. Comparison between the two-loop (short-dashed) and three-loop (solid) amplitude function of the order parameter. The resummed values [42] obtained using a Borel resummation are indicated by the dots for values of $N$ available.

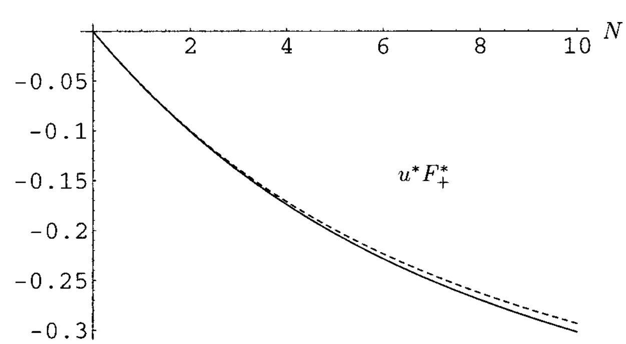


FIG. 8. Comparison between the strong-coupling limit of the two-loop (shot-dashed) and three-loop amplitude function (solid) $u^*F_+^*$.

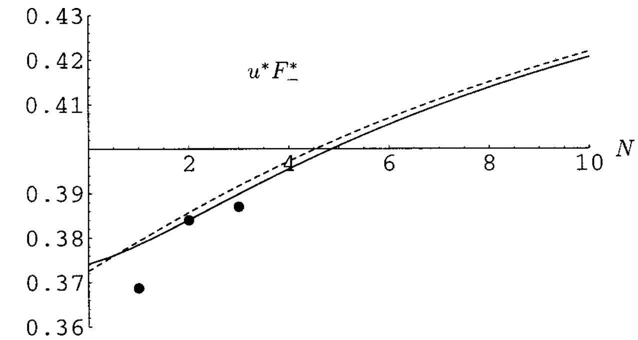


FIG. 9. Comparison between the strong-coupling limit of the two-loop (shot-dashed) and three-loop amplitude function (solid) $u^*F_-^*$. The resummed values [42] obtained using a Borel resummation are indicated by the dots for values of $N$ available.

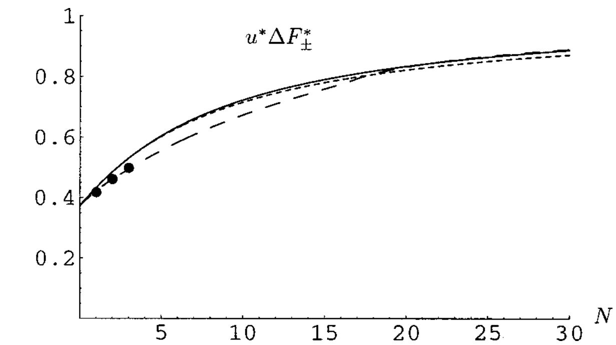


FIG. 10. Comparison between the strong-coupling limit of the two-loop (shot-dashed) and three-loop amplitude function (solid) $u^*\Delta F_\pm^* = u^*F_-^* - u^*F_+^*$. The three-loop (long-dashed) evaluation of $u^*(F_-^* - F_+^*)$ is in better agreement with the resummed values (dots) obtained in [42] using a five-loop ($N=1$) or three-loop ($N \neq 0$) Borel resummation.

$=0$. For the critical exponents, the signs of $\overline{f_1}$ and $f_3$ are the same because the series are alternating. For this reason, this equation has no real solution, and we must solve the turning-point equation $6f_3\hat{u}_B^*=0$, which is $\hat{u}_B^*=0$, leading to the optimized result $f^*=f_0$. For the amplitude functions, we have already seen that the alternating property is not necessarily true, so that the solution $\hat{u}_B^2 = -\overline{f_1}/(3f_3)$ is real. At the point where $f_2$ vanishes, we can see that the optimal value is

$$f^* = f_0 \pm \frac{2}{3}\overline{f_1}\sqrt{-\frac{2\overline{f_1}}{3f_3}} \qquad (135)$$

the positive or negative sign being chosen to get a continuity of the solution around $f_2$.

For the difference function $u(F_- - F_+)$, it is possible to follow exactly the strong-coupling limit as a function of $N$. Depending on $N$, there are four different solutions: below $\overline{N}_1 \approx 2.485\,27$ and above $\overline{N}_3 \approx 16.6066$, the argument of the square root of $r$ is negative, and one uses Eq. (25). For $N \in [\overline{N}_2, \overline{N}_3[$, one uses Eq. (24) with the positive root ($r=|r|$), where $\overline{N}_3 = -5+\sqrt{129} \approx 6.357\,82$ is the value of $N$ for which $f_2$ changes sign. The zero of $f_3$ lies within the same region. Finally, the last region is within the range $N \in ]\overline{N}_1, \overline{N}_2]$, for which we use Eq. (24), but with the negative root $r=-|r|$. More precisely,

$$u^*(F_-^* - F_+^*) = \frac{1}{2} + \frac{2(N-4)(N^2+10N-104)\rho(\rho+1)(2\rho-1)}{6[F_-^{(3)} - F_+^{(3)} + 24(7N^2-14N-440)]} \times \left(1-\frac{2}{3}r\right) - \frac{2[2(N^2+10N-104)]^3(2\rho-1)^3}{27[F_-^{(3)} - F_+^{(3)} + 24(7N^2-14N-440)]^2}(1-r), \qquad (136)$$

with $r=0$ for $N \lesssim \overline{N}_1$ and $N \gtrsim \overline{N}_3$, and $r$ the negative or positive square root of

$$r^2 = 1 - 3\,\frac{(N-4)[F_-^{(3)} - F_+^{(3)} + 24(7N^2-14N-440)]\rho(\rho+1)}{2[2(N^2+10N-104)]^2(2\rho-1)^2} \qquad (137)$$

for $N \in ]\overline{N}_1, \overline{N}_2]$ or $N \in [\overline{N}_2, \overline{N}_3[$, respectively.

Thus, the pole in $N$ of the two-loop approximation to $u^*(F_-^* - F_+^*)$ was only an artifact of the low order. At the three-loop level, the singularity is avoided by the interplay between the different possible solutions of Eq. (24) arising from the different branches of $r$: $r=0, \pm|r|$, with $|r|$ to be identified with the function $r$ defined below Eq. (24). This possibility was not exploited in previous works [2,5] because of the alternating signs for the critical exponents. [See, however, $\eta$ that required $r=-1$ for the strong-coupling limit of Eq. (74).]

In Fig. 10, we show the strong-coupling limit of $u^*(F_-^* - F_+^*)$. For comparison, we also give the direct difference $u^*\Delta F_\pm^*$ between $u^*F_-^*$ and $u^*F_+^*$, as obtained from Eqs. (133) and (132), as well as its two-loop counterpart (121). The range for $N$ has been increased to 30 in order to investigate the regions delimited by $\overline{N}_1$, $\overline{N}_2$, and $\overline{N}_3$.

For the direct difference, the changes brought about by the three-loop is very small, as before in Figs. 8 and 9. The difference between $u^*(F_-^* - F_+^*)$ and $u^*\Delta F_\pm^*$ is, however, somewhat larger. To facilitate the comparison, the following should be of help:

| $N$ | 0 | 1 | 2 | 3 | 4 |
|---|---|---|---|---|---|
| $u^*\Delta F_\pm^*$ (2 loops) | 0.372596 | 0.433608 | 0.485714 | 0.530258 | 0.568519 |
| $u^*\Delta F_\pm^*$ (3 loops) | 0.374166 | 0.432926 | 0.484899 | 0.530224 | 0.569615 |
| $u^*(F_-^*-F_+^*)$ (3 loops) | 0.374166 | 0.421864 | 0.461436 | 0.489995 | 1/2 |
| $u^*(F_-^*-F_+^*)$ (Ref. [41]) | | 0.4179 | 0.461 | 0.498 | |

The simple value 1/2 for the case $N=4$ comes from Eqs. (136) and (137): for $N=4$, $r$ is vanishing, meaning the third term of Eq. (136) does not contribute. Since the second term is also proportional to $N-4$, only the zero-loop order survives for the Higgs case. Our results for $u^*(F_-^*-F_+^*)$ are in good agreement with the Borel results of Ref. [41]. This is probably not a coincidence since we now resum the same function as they did. We note, however, that for the Ising model ($N=1$), we are not within the error bars of [41]. We have already noted this for the strong-coupling limit of $u^*F_-^*$.

Before closing the investigation of $u(F_- - F_+)$, we recall the case of $f_\Upsilon$, whose direct two-loop strong-coupling limit gave Eq. (111), exhibiting a pole. We know the strong-coupling limit should not have been far from $f_{\chi_T}^*/8$, see the discussion leading to Eq. (113). We have shown in this section how a pole in $u^*(F_-^*-F_+^*)$ at the two-loop level might disappear at the three-loop one. This is probably the case for $f_\Upsilon$. It would be very useful to get its three-loop order.

We can now turn to the strong-coupling limit of the renormalization group constant of the vacuum $B(u)$. Its three-loop value has been given in Eq. (101).

Upon inserting the relation between the renormalized and the bare coupling constant (14), we obtain

$$uB(u)=\frac{N}{2}\bar{u}_B-2N(N+8)\bar{u}_B^2+N(8N^2+167N+686)\bar{u}_B^3. \tag{138}$$

The series is alternating and behaves as for the critical exponents. No subtleties arise here as in the case of $f_\phi$ and $u^*(F_-^*-F_+^*)$. In particular, the argument of the square root of $r$ in Eq. (24) is negative for all $N$ and we have to work with Eq. (25). Using Eq. (25), the strong-coupling limit is

$$u^*B^*=\frac{N(N+8)\rho(\rho+1)(2\rho-1)}{6(8N^2+167N+686)}-\frac{16N(N+8)^3(2\rho-1)^3}{27(8N^2+167N+686)^2}. \tag{139}$$

This result is plotted in Fig. 11 together with the two-loop result $u^*N/2$, see Eq. (122). We also indicate the approximate result $u^*B^*=u^*N/2$ with $u^*$ from the three-loop expansion (84). There is no visible difference between the latter and Eq. (139).

To facilitate the comparison between the different approximations, we recapitulate the numerical results:

| $N$ | 0 | 1 | 2 | 3 | 4 |
|---|---|---|---|---|---|
| $u^*B^*$ (2 loops) | 0 | 0.0226337 | 0.04 | 0.0535312 | 0.0642361 |
| $u^*B^*$ (3 loops) | 0 | 0.0221074 | 0.0391089 | 0.0523643 | 0.0628447 |
| $u^*B^*=u_{(3)}^*N/2$ | 0 | 0.0219975 | 0.0388885 | 0.0520441 | 0.0624386 |
| $u^*B^*$ (Ref. [41]) | 0 | 0.020297 | 0.0363919 | 0.049312 | |

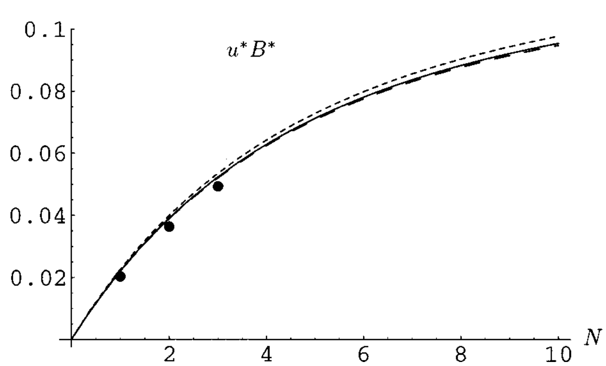


FIG. 11. Comparison between the strong-coupling limit of the two-loop (short-dashed) and three-loop (solid) renormalization group constant of the vacuum $u^*B^*$. For completeness, we also give the approximate three-loop (long-dashed) result $u_{(3)}^*N/2$. A five-loop calculation [41] using Borel resummation is included (dots) for values of $N$ available.

For the comparison with [41], we have multiplied their five-loop results for $B^*$ with their five-loop $u^*$. These five-loop results are within 7% from our three-loop strong-coupling calculation. This confirms that $B^*\approx N/2$ to all or-

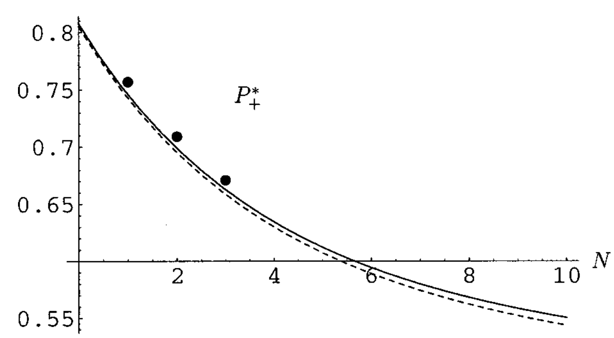


FIG. 12. Comparison between the strong-coupling limit of the two-loop (short-dashed) and three-loop (solid) polynomial $P_+^*$. The values [42] obtained using a five-loop Borel resummation are indicated by the dots for values of $N$ available.

ders. We shall, however, see in the next section that this 7% difference leads to a non-negligible difference in the universal combination $R_C$.

The next quantity we shall resum to three loops is the polynomial $P_+$. The three-loop bare expansion of the renormalized $P_+$ was given in Eq. (F4) and resummed to two loops in Eq. (123). The series in the bare coupling constant is alternating, and behaves as for the critical exponents. The strong-coupling limit of $P_+^*$ to three loops is then given by

$$P_+^* = 1 + \frac{9}{2}\frac{(N+2)(2N+17)\rho(\rho+1)(2\rho-1)}{[-3(36N^2+837N+3920)+24(N+8)\pi^2+4(43N+182)\ln(3/4)+288(N+8)\mathrm{Li}_2(-1/3)]} + 54\frac{(N+2)(2N+17)^3(2\rho-1)^3}{[-3(36N^2+837N+3920)+24(N+8)\pi^2+4(43N+182)\ln(3/4)+288(N+8)\mathrm{Li}_2(-1/3)]^2}, \tag{140}$$

with $\rho$ from Eq. (64).

In Fig. 12, we compare Eq. (140) with the two-loop result from Eq. (123). Almost no difference is found between our two- and three-loop expansions.

For a better comparison, we quote the numerical values for $N=0,1,2,3,4$:

| $N$ | 0 | 1 | 2 | 3 | 4 |
|---|---|---|---|---|---|
| $P_+^*$ (2 loops) | 0.805147 | 0.74269 | 0.695238 | 0.658642 | 0.63 |
| $P_+^*$ (3 loops) | 0.807683 | 0.745874 | 0.698901 | 0.662717 | 0.63447 |
| $P_+^*$ (Ref. [41]) | | 0.7568 | 0.7091 | 0.6709 | |

The two- and three-loop results agree within 1%. The results agree fairly well with the five-loop Borel resummation performed in [41]. We shall, however, see later that amplitude ratios depend crucially on the exact value of $P_+^*$. For this reason, our three-loop calculation is probably not precise enough. We shall present in the last section a numerical five-loop strong-coupling evaluation of $P_+^*$ to more firmly settle this statement.

To conclude this section, we discuss the amplitude of the susceptibilities above and below $T_c$ to three loops. We already know from the previous section that the two-loop amplitude above $T_c$ is identical to the order zero: $f_{\chi_+}^*=1$, see Eq. (108). As for the case of $uf_\phi$, we then expect a very small deviation from the zero-order value as well as a very smooth $N$ dependence. The series to evaluate in the strong-coupling limit is given in Eq. (C9). It is alternating and behaves like the series of the critical exponents. Moreover, with a vanishing linear term, but with a negative coefficient of the quadratic term, the solution of the optimalization problem is at variance with the case of the exponent $\eta$ or the amplitude $f_\phi$ if, as for these quantities, we admit that the solution is a maximum. From Eq. (127), we determine that the optimal value is $\hat{u}_B^*=0$, so that

$$f_{\chi_+}^*=1 \tag{141}$$

remains true at the three-loop level: The amplitude of the susceptibility above $T_c$ at the three-loop level does not depend on $N$. This is in contrast to [55], where a $N$-dependent fit, using Borel resummation, has been performed. Because our resummed value up to three loops is $f_{\chi_+}=1$, it is tempting to conjecture that this is true for all orders. However, contrary to the case of $\eta$ and $f_\phi$, we have here no argument to tell that the maximum has to be chosen instead of the minimum. Only when going to higher orders, then having more expansion coefficients, can we decide which solution is the right one. For this reason, we also mention below the other solution, which differs from unity for at most 2.5%:

$$f_{\chi_+}^* = 1 - \frac{48\,668(N+2)^3(2\rho-1)^3}{[27(N+2)(N+8)]^2[-113+12\pi^2+128\ln(3/4)+144\mathrm{Li}_2(-1/3)]^2}. \tag{142}$$

The comparison between the two curves is given in Fig. 13, as well as a comparison with the fit

$$f_{\chi_+} = 1-92(N+2)u^2(1+b_{\chi_+}u)/27 \tag{143}$$

taken from Table 1 of [55], with $b_\chi=9.68(N=1), 11.3\ (N=2)$, and $12.9\ (N=3)$, combined with the five-loop $u^*$ of Ref. [41]. More precisely, we have

| $N$ | 0 | 1 | 2 | 3 | 4 |
|---|---|---|---|---|---|
| $f^*_{\chi_+}$ (2 loops) | 1 | 1 | 1 | 1 | 1 |
| $f^*_{\chi_+}$ (3 loops) from (141) | 1 | 1 | 1 | 1 | 1 |
| $f^*_{\chi_+}$ (3 loops) from (142) | 0.979543 | 0.976298 | 0.975082 | 0.974977 | 0.975472 |
| $f^*_{\chi_+}$ (Refs. [41,55]) | | 0.976791 | 0.9748331 | 0.9740978 | |

The fact that our three-loop calculation (142) agrees very well with Refs. [41,55] might be an indication that Eq. (142) should be preferable to Eq. (141). However, from a variational perturbation theory point of view, nothing can be said. Only the determination of the next order might resolve the ambiguity.

Finally, we determine the strong-coupling limit of the amplitude of the susceptibility below $T_c$ for $N=1$. We have checked that the parameter $r$ in Eq. (24) is zero, i.e., we have to work with the turning-point equation (25). Applying it to Eq. (D4), we have

$$f^*_{\chi_-}=1+\frac{4352\rho(\rho+1)(2\rho-1)}{3[19\,904-11\,664c_1+3\pi^2+10\,480\ln(4/3)+36\mathrm{Li}_2(-1/3)]}-\frac{164\,852\,924\,416(2\rho-1)^2}{19\,683[19\,904-11\,664c_1+3\pi^2+10\,480\ln(4/3)+36\mathrm{Li}_2(-1/3)]^2}, \tag{144}$$

with $\rho$ from Eq. (64). Numerically, this is evaluated as $f^*_{\chi_-}\approx 2.09387$, to be compared with the two-loop result (124) $211/103\approx 2.048\,544$. They agree within 3%.

For the ratio (105), the calculation of $f_{\chi_-}/f_{\chi_+}$ is needed. Its strong-coupling limit can be determined using the individual strong-coupling limit of the numerator and the denominator. In that case, the ambiguity on $f^*_{\chi_-}$ at the three-loop level is relevant. According to the choice $f^*_{\chi_+}=1$ from Eq. (141) or $f^*_{\chi_+}\approx 0.976\,298$ from Eq. (142) with $N=1$, we have

$$\frac{f^*_{\chi_-}}{f^*_{\chi_+}}=2.093\,87, \tag{145}$$

$$\frac{f^*_{\chi_-}}{f^*_{\chi_+}}=2.1447, \tag{146}$$

respectively.

The strong-coupling limit of the ratio $f_{\chi_-}/f_{\chi_+}$ can also be computed from its perturbative expansion. It has been derived in Appendix D, see Eq. (D6). The strong-coupling limit reads

$$\left(\frac{f_{\chi_-}}{f_{\chi_+}}\right)^*=1+\frac{1420\rho(\rho+1)(2\rho-1)}{3[19\,184-11\,664c_1+99\pi^2+9456\ln(4/3)+1188\mathrm{Li}_2(-1/3)]}-\frac{5\,726\,576\,000(2\rho-1)^2}{729[19\,184-11\,664c_1+99\pi^2+9456\ln(4/3)+1188\mathrm{Li}_2(-1/3)]^2}. \tag{147}$$

Its numerical value is 2.112 27, to be compared with the two-loop result (125) $751/355\approx 2.115\,49$. The three-loop level is in very good agreement with the two-loop result, within less than 0.2%. However, this by no means signify that the asymptotic limit has been reached, and the ratios (145) or (146) might be closer to the true ratio than Eq. (147). This is due to the fact that the even and odd orders are on different converging lines because odd (even) terms come from an extremum (turning-point) condition or vice versa. To see the speed of convergence, it would be necessary to compare the four-loop order with the two-loop order, and the five-loop order with the three-loop order.

### E. Amplitude ratios from two- and three-loop expansions

We have now everything in hand in order to compute the ratio of the heat capacity $A^+/A^-$, the universal combination $R_C$, and the ratio of the susceptibilities $\Gamma_+/\Gamma_-$. This section is restricted to a full two- and three-loop calculation. In order to improve the ratios, we shall break our rule of being

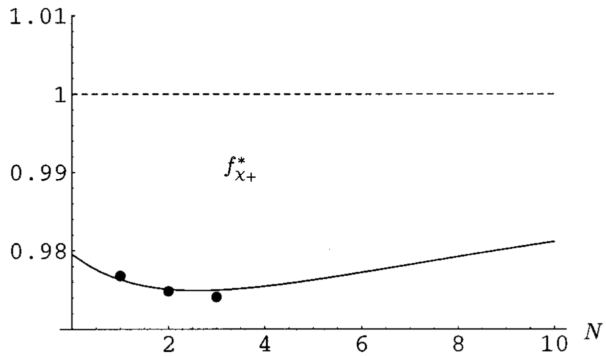


FIG. 13. Comparison between the two-loop strong-coupling limit (short-dashed) of the amplitude $f^*_{\chi_+}$ of the susceptibility above $T_c$ and the second possible solution (142) at the three-loop level (solid). The values [55] obtained using a five-loop Borel resummation (dots) are given for values of $N$ available.

self-consistent in the next section and use there the maximum information available.

We start with the heat capacity $A^+/A^-$. Since we have a preference for Eq. (100) over Eq. (118), we shall work with the separate strong-coupling limit evaluation of $u^*F^*_-$ and $u^*F^*_+$. We have checked that the effect on the ratio $A_+/A_-$ is negligible. The exponent $\alpha$ entering it is calculated from the two- or three-loop result for $\nu$ given in Eq. (52) and Eq. (81), respectively, using the hyperscaling relation $\alpha = 2 - D\nu$.

Combining the different results derived previously, we have

| $N$ | 0 | 1 | 2 | 3 | 4 |
|---|---|---|---|---|---|
| $A_+/A_-$ (2 loops) | 0 | 0.489106 | 0.843065 | 1.12691 | 1.37015 |
| $A_+/A_-$ (3 loops) | 0 | 0.491088 | 0.862 439 | 1.16719 | 1.43243 |

Regarding the fact that the critical exponent $\alpha$ is far away from its asymptotic limit (it is still positive for $N=2$, while the shuttle experiment [28] shows clearly a negative value), the results of this table are promising: For $N=2$, we obtain $A_+/A_- \approx 0.862439$ at the three-loop level, while the shuttle experiment [28] gives $A_+/A_- \approx 1.0442$, see Eq. (1). We shall see in the next section that working with asymptotic critical exponents leads to a better agreement with experiments.

The next ratio we examine is Eq. (104), the universal combination $R_C$. The results are best displayed as

| $N$ | 0 | 1 | 2 | 3 | 4 |
|---|---|---|---|---|---|
| $R_C$ (2 loops) | 0 | 0.062474 | 0.124819 | 0.184355 | 0.239967 |
| $R_C$ (3 loops, $f^*_{\chi_+}=1$) | 0 | 0.05944 | 0.121628 | 0.182413 | 0.239691 |
| $R_C$ (3 loops, $f^*_{\chi_+}$ from (142)) | 0 | 0.060883 | 0.124736 | 0.187094 | 0.245718 |

We see an overall agreement between the two- and three-loop results. We have also checked that the ratio $R_C$ calculated with the formula (103) used in [42] is within less than 1%. Moreover, our results are in agreement with the values $R_C(N=2)=0.123$ and $R_C(N=3)=0.189$ given in Ref. [42]. Since we expect that using the true critical exponent will lead to a better ratio $A_+/A_-$, it is important to see how $R_C$ evolves. Will the agreement with [42] be lost? This issue is investigated in the next section.

To end this section, we study the ratio of the susceptibilities $\Gamma_+/\Gamma_-$ for the Ising model, see Eq. (105).

The two-loop result for the amplitude ratio (105) is, with $\nu = 56/90$ from Eq. (52), with $P^*_+ = 127/171$ from Eq. (123) and with $f^*_{\chi_+}=1$:

$$\frac{\Gamma_+}{\Gamma_-} = \frac{211}{103}\left(\frac{4\nu P^*_+}{3-4\nu P^*_+}\right)^{2\nu} = \frac{211}{103}\left(\frac{14\,224}{8861}\right)^{56/45} \approx 3.691\,71. \tag{148}$$

This is still far from the value $\approx 4.7$ quoted in the literature [18,56]. A small improvement is obtained using the direct strong-coupling evaluation of $f_{\chi_-}/f_{\chi_+}$ of Eq. (125):

$$\frac{\Gamma_+}{\Gamma_-} = \frac{751}{355}\left(\frac{4\nu P^*_+}{3-4\nu P^*_+}\right)^{2\nu} = \frac{751}{355}\left(\frac{14\,224}{8861}\right)^{56/45} \approx 3.812\,36. \tag{149}$$

This value is still far from the expected ratio 4.7. However, the ratio depends sensibly on the value of the critical exponent $\nu$. For example, using $\nu = 0.63$, we increase Eq. (149) to $\Gamma_+/\Gamma_- = 4.002$. The sensibility is also seen when calculating the three-loop value of the ratio:

$$\frac{\Gamma_+}{\Gamma_-} \approx 3.887\,85, \tag{150}$$

where the ratio $(f_{\chi_-}/f_{\chi_+})^*$ has been obtained from (147).

### F. Amplitude ratios using maximum information

Up to now, we have followed the strategy to make a fully consistent two- and three-loop calculation. The comparison between the two- and three-loop amplitude functions has made us believe that the resummed values are close to the extrapolated limit $L \to \infty$, although one has to take care that odd and even approximations are on different converging lines. For the critical exponents, it is primordial going to the asymptotic limit. For example, we have $\alpha(N=2)$ still positive at the three-loop level, while the shuttle experiment, see second reference of [28] and Eq. (1), shows a value of $\alpha(N=2) = -0.010\,56$.

In this section, we shall relax our constrain of working only with two- and three-loop quantities and will take the maximum available information, i.e., our three-loop result for the amplitudes and extrapolated, or experimental, value for the critical exponents. We shall also see the effect of using $uB$ to five loops.

Except for $\alpha(N=2)$ that we took from the shuttle experiment [28], the exponents are taken from the $D=3$ tables of [18], i.e., we are working with, for $N=0,1,2,3,4$:

$$\nu=0.5882 \quad 0.6304 \quad 0.6703 \quad 0.7073 \quad 0.741$$

$$\alpha=0.235 \quad 0.109 \quad -0.010\,56 \quad -0.122 \quad -0.223. \tag{151}$$

Combining the three-loop strong-coupling limit of the amplitudes performed in Sec. IV D with these exponents, we obtain, for $A_+/A_-$,

| $N$ | 0 | 1 | 2 | 3 | 4 |
|---|---|---|---|---|---|
| $A_+/A_-$ | 0 | 0.543406 | 1.04516 | 1.54386 | 2.0444 |
| $A_+/A_-$ (Ref. [41]) | 0 | 0.540 | 1.056 | 1.51 | |

We have checked that the increase from the three-loop value (for $N=2$, this ratio was 0.862 439) is mainly due to using the correct $\alpha$. For example, with the correct $\alpha$ but still using the three-loop $\nu$ of Eq. (81), we would have obtained, for $N=2$, a ratio 1.047 11. It also does not depend too sensitively on using the five-loop strong-coupling limit of $u^*B^*$ and $P_+^*$, neither on using $u^*(F_-^*-F_+^*)$ instead of the separate calculation of $u^*F_-^*$ and $u^*F_+^*$. For example, playing with all these quantities, the ratio, for $N=2$, could be changed from $A_+/A_-=1.045\,16$ to, at most, $A_+/A_-=1.049$, depending on which quantities are taken to five loops. A complete numerical study of this ratio, using variational perturbation theory up to five loops, will be presented elsewhere [58].

For $N=2$, our result 1.045 16 coincides remarkably well with the shuttle experiment, see second reference of [28]. For $N=1$, we have 0.543 406, which agrees reasonably well with Ref. [25] ($A_+/A_-\approx 0.541$) and with the values quoted in Table 5 of [18], values that are both experimental and theoretical. In Ref. [41], the authors obtained 1.056 for $N=2$. Their Table 4 makes a comparison between their result and other works and experiments, for $N=1,2,3$. We see that the agreement is good. In our table, we have listed only the values calculated in the work [41] since the model is the same.

For the universal combination $R_C$, we obtain, using the five-loop critical exponents (151) and the three-loop amplitudes of Sec. IV D

$$R_C=0,\ 0.061\,625\,7,\ 0.130\,341,\ 0.201\,404,\ 0.270\,882 \tag{152}$$

for $N=0,1,2,3,4$.

Here also, we have checked that the main effect is due to choosing the correct $\alpha$. Working with $\nu$ at the three-loop level only modifies the result slightly. While working with the true exponents for the ratio $A_+/A_-$ had considerably improved it, making it coincide with the experimental values, we see for $R_C$ that the values of the previous section, with a wrong $\alpha$ were in better agreement with the quoted values in [42]: $R_C=0.123,0.189$ for $N=2,3$, respectively. We have checked that our result for $N=2$ is not changed if we take the values of $\alpha$ and $\nu$ taken in [42]. Also, the result does not depend sensibly on $u^*F_+^*$, although our value differs from theirs. We have traced back the difference between our result and [41] to $uB$ at the critical point: limiting ourselves to $N=2$, we have $u^*B^*\approx 0.039\,108\,9$ while [41] gives a value $u^*B^*\approx 0.036\,391\,9$. This difference is all that is needed to explain the difference between our result and the result of Ref. [42], apart from a very small difference coming also from our use of Eq. (104) instead of Eq. (103). Since $u^*B^*$ has been obtained in [41] using a five-loop Borel resummation, it is tempting to believe it is more accurate. For this reason, we have also determined numerically the five-loop strong-coupling limit of $uB$. We shall show a detailed numerical resummation in [58], showing here only the main steps. Starting from the five-loop expansion [41,43]

$$uB(u)=\frac{N}{2}u+\frac{N(N+2)}{48}u^3+\frac{N(N+2)(N+8)[-25+12\zeta(3)]}{648}u^4+N(N+2)$$
$$\times\frac{[-319N^2+13\,968N+64864+16(3N^2-382N-1700)\zeta(3)+96(4N^2+39N+146)\zeta(4)-1024(5N+22)\zeta(5)]}{41472}u^5, \tag{153}$$

and using the algorithm given by Eq. (17), the corresponding strong-coupling limit is

| $N$ | 0 | 1 | 2 | 3 | 4 |
|---|---|---|---|---|---|
| $u^*B^*$ (5 loops) | 0 | 0.0209552 | 0.0372717 | 0.0502225 | 0.0605918 |
| $u^*B^*$ (Ref. [41]) | 0 | 0.020297 | 0.0363919 | 0.049312 | |

Our five-loop result is now much nearer to the Borel resummed values of [41] than our three-loop order of Sec. IV D. For this reason, we believe our five-loop result is near the infinite-loop limit extrapolation. More details will be given in [58], which also contains the effect of variations of $P_+^*$, which is the second source, after $u^*B^*$, of error for $R_C$.

Finally, our best values for the ratio $R_C$ are collected

| $N$ | 0 | 1 | 2 | 3 | 4 |
|---|---|---|---|---|---|
| $R_C$ | 0 | 0.05803 | 0.12428 | 0.19402 | 0.26285 |
| $R_C$ (Ref. [41]) | 0 | | 0.123 | 0.189 | |

To our knowledge no experimental value of this ratio is known for $N=2$. The case $N=3$ is presented in Table 7.6 of Ref. [56]. For $N=1$, the value of the ratio has only slightly changed compared to the results based on three-loop $\alpha$ and $\nu$. This is due to the fact that, for $N=1$, $\alpha$ is positive and its effect on $R_C$ is less sensitive. In the work [18], the theoretical and experimental values of $R_C$ are also given for $N=1$. The theoretical values seem to prefer a value around 0.057 while the experimental values are around 0.050. From Table 7.1 of [56] we, however, see that values close to 0.06 might as well be obtained. A result ($R_C \approx 0.0594$) close to this latter value was also obtained theoretically in [25].

Better experiments or other theoretical studies are needed in order to see if our predictions are correct or have to be ruled out.

Finally, we conclude this section with the ratio of the susceptibilities for the Ising model. Using the critical exponent $\nu$ to five loops Eq. (151), we obtain

$$\Gamma_+/\Gamma_- = 4.06419, \tag{154}$$

where we took the ratio $(f_{\chi_-}/f_{\chi_+})^*$ from Eq. (147). We might have slightly increased $\Gamma_+/\Gamma_-$ using the value 2.1447 of Eq. (146). However, we would still be far from the value 4.77 of [18], the value confirmed in the work [25]. The only possible quantity we may still vary in the ratio (105) is $P_+^*$. Our three-loop value is 0.745 874, while the five-loop result given in [41] using Borel resummation is 0.7568. Using this value in our formula for the ratio, we find

$$\Gamma_+/\Gamma_- = 4.271\,54. \tag{155}$$

The ratio of the susceptibilities depends sensitively on $P_+^*$. We postpone to [58] the application of variational perturbation theory up to five loops for the resummation of $P_+^*$ and $\Gamma_+/\Gamma_-$. We do not, however, expect a resummed $P_+^*$ different from [41]. For this reason, the ratio (155) is probably the best we can obtain. A ratio of 4.77 obtained in [18] and references therein seem to be ruled out from our analysis.

## V. CONCLUSION

In this paper, we have shown that variational strong-coupling theory [2,5] can be applied not only to critical exponents, but also to various amplitude ratios. We have focused on two- and three-loop results were analytical results for the amplitude functions are known [41,42,46] for all $N$ both above and below $T_c$. Our results are analytical expressions, except in the last section where we used more information to find $A_+/A_-$, $R_C$ and $\Gamma_+/\Gamma_-$. The results are quite sensitive to the precise value of the critical exponents. In addition, a five-loop evaluation of the renormalization constant $B^*$ was necessary. The ratio $R_C$ was so sensitive to it that a three-loop calculation was not sufficient. The same remark holds for $P_+^*$, which affects mainly $\Gamma_+/\Gamma_-$. A numerical study of the known five-loop amplitudes will be done in [58], which will contain refined results compared to Sec. IV F.

One interesting observation of our work is that we can evaluate series that have caused problems in previous Borel resummations when the expansion coefficients in terms of the renormalized coupling constant are not alternating to low orders. For these functions, the strong-coupling theory turned out to work well.

Having obtained analytical expressions in $N$, we have shown that the coefficient of the series in the bare coupling constant may vanish and change sign. At the two-loop level, this lead to diverging results near certain value of $N$. We have seen that the problem disappears at the three-loop level, because of the interplay of the different coefficients of the series. We could show precisely how it works because all our results were analytical and not restricted to integer values of $N$.

When using variational perturbation theory, nothing is known of the nature of the optimal variational parameter, which can be a minimum, a maximum, or a turning point. The analysis performed here should help to identify the correct (numerical) solution at higher-loop order. See for example the amplitude $f_{\chi_+}^*$, for which it is not yet clear which of the solutions (141) or (142) has to be chosen.

## ACKNOWLEDGMENTS

We are grateful to Dr. C. Bervillier for several interesting clarifications. We thank also Dr. B. Kastening, Dr. F. Nogueira, and Dr. A. Pelster for valuable discussions during the completion of this work and M. Bachmann for help speeding up the calculations. The work of B.VdB. was supported by the Alexander von Humboldt foundation and the FNRS (Belgium).

## APPENDIX A: EXPONENT $\omega$ FROM STRONG-COUPLING THEORY

The power $p/q$ of the leading power behavior $\overline{u}_B^{p/q}$ of a function $W_L$ whose perturbative expansion has been given in Eq. (20) can be obtained taking the logarithmic derivative, giving Eq. (21). A subtlety arises for functions going to a constant in the strong-coupling limit. For such functions, $p$ vanishes and the corresponding $f^*$ in Eq. (17) vanishes. Care has to be taken: the limit $f^* \to 0$ is different from imposing $f^*=0$. In the former case, we can identify $q$ (or $\omega$) by matching the series to achieve $f^*=0$. Working directly with a series that has $f^*=0$ implies a leading behavior $p'/q = -\omega/\epsilon$. The algorithm (17) serves then to identify the coefficient $c_0$ of the rhs of Eq. (18). As an example of how to use the series, let us derive the relation [2,5,13]

$$-\frac{\omega}{\epsilon} - 1 = \frac{d \ln W_L'}{d \ln \overline{u}_B}. \tag{A1}$$

The left-hand side is of the type of Eq. (18), and the algorithm (17) can be applied. Formula (A1) follows directly from Eq. (18). Alternative derivation starts from Eq. (21): If $p/q$ is vanishing, this means that its series has a leading exponent $p'/q=-\omega/\epsilon$, which we derive in the following manner. Start from formula (21) with its exponent $p'/q$ that we know from the general behavior (18) with $f^*\equiv p/q=0$, i.e.,

$$\frac{p'}{q}=-\frac{\omega}{\epsilon}=\frac{d\ln(p/q)}{d\ln \overline{u}_B} \tag{A2}$$

where $p/q$ is not yet taken at its asymptotic zero value, but is given as the right-hand-side of Eq. (21). It then follows

$$-\frac{\omega}{\epsilon}=1+\overline{u}_B\left(\frac{W_L''}{W_L'}-\frac{W_L'}{W_L}\right)=1+\overline{u}_B\frac{W_L''}{W_L'}-\frac{p}{q}. \tag{A3}$$

Taking the limit $\overline{u}_B\to\infty$, the term $p/q$ vanishes by hypothesis, and we end up once more with formula (A1).

Although the algorithm (17) cannot be applied directly for the right-hand side of Eq. (21) if $p/q$ is vanishing exactly but only in the limit $p/q\to 0$, we can, nevertheless, use a trick to circumvent this problem: If the series for $W_L$ has a vanishing leading power $p/q$, then $W_L/\overline{u}_B$ has a power $p'/q=-1$. This allows us to deduce

$$\frac{p'}{q}\equiv-1=\frac{d\ln(W_L/\overline{u}_B)}{d\ln\overline{u}_B}=\overline{u}_B\frac{W_L'}{W_L}-1=\frac{p}{q}-1. \tag{A4}$$

This shows that the right-hand-side of Eq. (21) can be used to reach the limit 0. Then, $\omega$ can be extracted either from Eq. (21) or from Eq. (A1). It is also clear from the expression (A3) that the right-hand-side has to be resummed blockwise: we have to use the intermediate result $p/q=0$ before tempting to resum. Using a full resummation of the right-hand-side of the latter equation would lead to badly resummed results (although the underlying $\epsilon$ expansion would be the same): It is necessary to use $p/q=0$ in Eq. (A3), and not its analytical form that would have been mixed up with the power series of $W_L''/W_L'$.

## APPENDIX B: FREE ENERGY TO THREE LOOPS

From the model Hamiltonian (4), the analytical calculation of the Gibbs free energy $\Gamma_B(m'^2_B,u_B,M_B)$ near the coexistence curve below $T_c$ and for $M_B^2\equiv\langle\phi_B^2\rangle=0$ above $T_c$ has been obtained at the two-loop order in [46] and at the three-loop order in [41], thus extending the $N=1$ calculation of Rajantie [35]. We write directly the three-loop result:

$$\Gamma_B=\frac{1}{2}m'^2_BM_B^2+u_BM_B^2+\sum_{b=1}^{3}\sum_{l=0}^{b-1}\sum_{k=0}^{1}(-1)^k2^{-l-k}F_{blk}(\overline{\omega},N)\times(24u_B)^{3-l}(M_B^2)^l\left[\frac{r_{0L}}{(24u_B)^2}\right]^{(4-b-2l)/2}\ln\left[\frac{r_{0L}}{(24u_B)^2}\right]^k, \tag{B1}$$

where $r_{0L}=m'^2_B+12u_BM_B^2$ is the longitudinal bare mass, the transverse one $r_{0T}=m'^2_B+4u_BM_B^2$ being included in the parameter $\overline{\omega}=r_{0T}/r_{0L}$. The nonanalyticity in the coupling constant is seen in the last term.

The functions $F_{blk}$ can be found in [41,46]. Since we need them later on in this Appendix, we shall write the nonzero components:

$$F_{100}=-\frac{1}{12\pi}[1+(N-1)\overline{w}^{3/2}], \tag{B2}$$

$$F_{200}=\frac{1}{384\pi^2}[3+2(N-1)\overline{w}^{1/2}+(N^2-1)\overline{w}], \tag{B3}$$

$$F_{210}=\frac{1}{288\pi^2}(N-1)\ln\frac{1+2\overline{w}^{1/2}}{3}, \tag{B4}$$

$$F_{211}=-\frac{1}{288\pi^2}(N+2). \tag{B5}$$

$$F_{300}=\frac{1}{18\,432\pi^3}\Bigg(15+24\ln\tfrac{3}{4}-(N-1)\Bigg\{\overline{w}^{-1/2}+2N-6+8\ln\frac{2+2\overline{w}^{1/2}}{3}+\overline{w}^{1/2}\Bigg[N^2-6N-9+4(N+1)\ln\frac{16\overline{w}}{9}+8\ln\frac{2+2\overline{w}^{1/2}}{3}\Bigg]+\overline{w}(N-1)\Bigg\}\Bigg), \tag{B6}$$

$$F_{301}=\frac{1}{2304\pi^3}\{3+(N-1)[1+(N+2)\overline{w}^{1/2}]\}, \tag{B7}$$

$$F_{310}=\frac{1}{27\,648\pi^3}(9\pi^2-18+108\mathrm{Li}_2(-\tfrac{1}{3})-(N-1)\{4\overline{w}^{-1/2}+4N+2-(N+2)\pi^2-12\mathrm{Li}_2(\tfrac{1}{3})-32\ln 2-6(\ln 3)^2+\overline{w}^{1/2}[10N+32-16(2N+3)\ln 2+48\ln 3-8(N+1)\ln\overline{w}]+\tfrac{1}{3}\overline{w}(84N-100-128\ln 2)\}), \tag{B8}$$

$$F_{320}=\frac{1}{165\,888\pi^3}\Bigg[432\ln\tfrac{4}{3}-324\mathrm{Li}_2(-\tfrac{1}{3})-432c_1-27\pi^2-(N-1)\Bigg(16\overline{w}^{-1/2}+\frac{3N+14}{3}\pi^2+18(\ln 3)^2+36\mathrm{Li}_2(\tfrac{1}{3})+16[c_2+4\mathrm{Li}_2(-2)-2\mathrm{Li}_2(-\tfrac{1}{2})+(6\ln 3-\ln 2-\tfrac{13}{3})\ln 2]-\tfrac{128}{3}+16\overline{w}^{1/2}[7-N+(N+1)\ln(16\overline{w})+2\ln 2-6\ln 3]+4\overline{w}\{4c_2-12N-\tfrac{224}{5}+\pi^2+6(6\ln 3-\ln 2-\tfrac{16}{15})\ln 2+12[2\mathrm{Li}_2(-2)-\mathrm{Li}_2(-\tfrac{1}{2})]]\}\Bigg)\Bigg], \tag{B9}$$

where, in the coefficients $F_{310}$ and $F_{320}$ below $T_c$, terms of order $O(\overline{w}^{3/2},\overline{w}^{3/2}\ln\overline{w})$ have been neglected (the coefficients are calculated in the vicinity of the coexistence curve where an expansion with respect to $\overline{w}$ is justified). The constants $c_1$ and $c_2$ have been defined in the main text, see Eqs. (96) and (97).

Inverting the equation of state

$$h_B=\frac{\partial}{\partial M_B}\Gamma_B \tag{B10}$$

gives, in the limit $h_B\to 0$, and to this order, the square of the magnetization:

$$\begin{aligned}M_B^2=&\frac{1}{8u_B}(-2m'^2_B)+\frac{3}{4\pi}(-2m'^2_B)^{1/2}+\frac{u_B}{8\pi^2}\left[10-N+4(N-1)\ln 3-2(N+2)\ln\frac{-2m'^2_B}{(24u_B)^2}\right]+\frac{u_B^2(-2m'^2_B)^{-1/2}}{1920\pi^3}\\&\times\Bigg\{-2736N-5904-6480c_1+240(N-1)c_2\\&-(75N^2-5N+875)\pi^2-1260[(N-1)\mathrm{Li}_2(\tfrac{1}{3})\\&+9\mathrm{Li}_2(-\tfrac{1}{3})]+960(N-1)[2\mathrm{Li}_2(-2)-\mathrm{Li}_2(-\tfrac{1}{2})]\\&-630(N-1)(\ln 3)^2-48\ln 2[10(N-1)\ln 2\\&-60(N-1)\ln 3+111N-561]+240(12N-57)\\&\times\ln 3-1440(N+2)\ln\frac{-2m'^2_B}{(24u_B)^2}\Bigg\}.\end{aligned} \tag{B11}$$

The logarithmic terms in $u_B$ are nonanalyticities that can be removed using the length $\xi_-$ instead of $m'^2_B<0$, see [38]. Up to the three-loop order, the relation between $\xi_-$ and $m'^2_B<0$ is

$$\begin{aligned}-2m'^2_B=&\xi_-^{-2}\Bigg\{1+\frac{N+2}{\pi}u_B\xi_- -\frac{N+2}{\pi^2}(u_B\xi_-)^2[\tfrac{1385}{108}\\&+4\ln(24u_B\xi_-)]+\frac{N+2}{108\pi^3}(u_B\xi_-)^3\\&\times\Bigg[3(438N+4349)+576(N+8)\mathrm{Li}_2(-\tfrac{1}{3})\\&+48(N+8)\pi^2+8(43N+182)\ln\frac{3}{4}\Bigg]\Bigg\}.\end{aligned} \tag{B12}$$

Using Eq. (B12) in Eq. (B11) one obtains an analytic function of $u_B$, from which one extract the amplitude $f_\phi$ of Eqs. (85) and (93), after proper normalization with the help of $Z_\phi$. This has been done in [42,46] and will not be repeated here. The equations we have quoted here are mentioned because we shall need them below for obtaining the amplitude functions $f_{\chi_+}$ and $f_{\chi_-}$ which, to our knowledge, have not been determined analytically within this model.

## APPENDIX C: THREE-LOOP AMPLITUDE FUNCTION OF THE ISOTROPIC SUSCEPTIBILITY ABOVE $T_C$

By definition, the amplitude of the susceptibility above $T_c$ is obtained from the susceptibility at zero momentum $f^B_{\chi_+}=\xi_+^2\chi^{-1}_{+,B}$, where the inverse susceptibility is given by the two-point function $\Gamma^{(2)}_B$ at zero momentum. The correlation length above the critical temperature $\xi_+$ is defined as in Refs. [41,42,46]:

$$\xi_+^2=\chi_{+,B}(q)\,\partial\chi^{-1}_{+,B}(q)/\partial q^2|_{q^2=0}. \tag{C1}$$

Combining with the definition of $f^B_{\chi_+}$, we have

$$f^B_{\chi_+}=\left.\frac{\partial\chi^{-1}_{+,B}}{\partial q^2}\right|_{q^2=0}=\left.\frac{\partial\Gamma^{(2)}_B}{\partial q^2}\right|_{q^2=0}. \tag{C2}$$

The derivative of $\Gamma^{(2)}_B$ with respect to $q^2$ is needed. This is in contrast to Refs. [41,42,46] where only the combination (C1) was needed. For this reason, the intermediate result leading to Eq. (C2) was not published. Being needed to determine the ratio $R_C$ in Eq. (104) and the ratio of the susceptibilities (105), we derive it in the following. The two-point function can be written as $\Gamma^{(2)}_B=r_0+q^2-\Sigma_B(q,r_0,\overline{u}_B)$, where the self-energy has the expansion $\Sigma_B(q,r_0,\overline{u}_B)=\Sigma_{m=1}^{\infty}(-\overline{u}_B)^m\Sigma^{(m)}_B(q,r_0)$. The two-loop results have first been given in Appendix A of Ref. [46], with the result, up to order $q^2$:

$$\begin{aligned}\Gamma^{(2)}=&q^2+r_0-4(N+2)A_Du_Br_0^{1/2}+8(N+2)^2A_D^2u_B^2\\&-32\frac{(N+2)}{(4\pi^3)}\left[\frac{2\pi}{D-3}-\frac{2\pi}{27}\frac{q^2}{r_0}\right]u_B^2.\end{aligned} \tag{C3}$$

The pole at $D=3$ can be eliminated by subtraction, leading to the masses $m_B^2$ and $m'^2_B$. This is, however, of no concern here since we are interested in taking the derivative with respect to $q^2$:

$$\left.\frac{\partial\Gamma^{(2)}_B}{\partial q^2}\right|_{q^2=0}=1+\frac{N+2}{27\pi^2}\frac{u_B^2}{r_0}. \tag{C4}$$

For the three-loop expansion, one must calculate the diagrams in Appendix B of [42]. Again, we concentrate on the derivative of the susceptibility at zero momentum, focusing on the diagrammatic Eq. (B5) of [42]. The corresponding vacuum diagrams have been given by Rajantie in [35], see in particular its Eqs. (15) and (25) and, taking the appropriate derivative with respect to the mass, we obtain the contribution of the three-loop diagrams:

$$\left.\frac{\partial\Sigma_B^{(3)}}{\partial q^2}\right|_{q^2=0}=\left\{\frac{(N+2)^2}{27\pi^3}-\frac{(N+2)(N+8)}{54\pi^3}[-8+3\pi^2+32\ln\tfrac{3}{4}+36\mathrm{Li}_2(-\tfrac{1}{3})]\right\}r_0^{-3/2}. \tag{C5}$$

This has to be combined with Eq. (C4) to yield the expansion

$$\left.\frac{\partial\Gamma_B^{(2)}}{\partial q^2}\right|_{q^2=0}=1+\frac{N+2}{27\pi^2}\frac{u_B^2}{r_0}+\left\{\frac{(N+2)^2}{27\pi^3}-\frac{(N+2)(N+8)}{54\pi^3}\times[-8+3\pi^2+32\ln\tfrac{3}{4}+36\mathrm{Li}_2(-\tfrac{1}{3})]\right\}\frac{u_B^3}{r_0^{3/2}}. \tag{C6}$$

Since there is no linear term $u_B$, the amplitude of the susceptibility above $T_c$ to three loops requires only the one-loop order of the correlation-length $\xi_+$, i.e., the one-loop order of the susceptibility. To three loops, the following expression

$$m'^2_B=\xi_+^{-2}\left\{1+\frac{N+2}{\pi}u_B\xi_++\frac{N+2}{\pi^2}(u_B\xi_+)^2\times\left[\frac{1}{27}+2\ln(24u_B\xi_+)\right]+\frac{N+2}{\pi^3}(u_B\xi_+)^3\times[3(3N+22)-144(N+8)\mathrm{Li}_2(-\tfrac{1}{3})-12(N+8)\pi^2-2(43N+182)\ln\tfrac{3}{4}]\right\} \tag{C7}$$

is found in the literature, see [42]. This is the analog of Eq. (B12) above $T_c$. At the one-loop level, there is no distinction between $r_0$ and $m_B^2$, and we identify $r_0=\xi_+^{-2}[1+(N+2)u_B\xi_+/\pi]$. Together with Eq. (C6), we arrive at

$$f_{\chi_+}^B\equiv\left.\frac{\partial\Gamma_B^{(2)}}{\partial q^2}\right|_{q^2=0}=1+\frac{N+2}{27\pi^2}(u_B\xi_+)^2-\frac{(N+2)(N+8)}{54\pi^3}\times[-8+3\pi^2+32\ln\tfrac{3}{4}+36\mathrm{Li}_2(-\tfrac{1}{3})](u_B\xi_+)^3. \tag{C8}$$

This has to be compared with the numerical coefficients $a_m^{(2)}$ of Table 2 in [55].

Having calculated the bare amplitude function $f_{\chi_+}^B$, we can now turn to the normalized one $f_{\chi_+}$. Since the latter is related to a two-point function, the normalization factor is equal to the wave-function renormalization constant $Z_\phi$: $f_{\chi_+}=Z_\phi f_{\chi_+}^B$, with $Z_\phi$ being supplied by Eq. (16). Using the relation (13) between $u_B$ and $\overline{u}_B=u_B\xi_+/(4\pi)$, we arrive at the normalized amplitude function of the susceptibility above $T_c$, expressed in terms of the reduced bare coupling constant $\overline{u}_B$:

$$f_{\chi_+}=1-\tfrac{92}{27}(N+2)\overline{u}_B^2-\tfrac{8}{27}(N+2)(N+8)\times[-113+12\pi^2+128\ln\tfrac{3}{4}+144\mathrm{Li}_2(-\tfrac{1}{3})]\overline{u}_B^3. \tag{C9}$$

The corresponding expansion in terms of the renormalized coupling constant gives

$$f_{\chi_+}=1-\tfrac{92}{27}(N+2)u^2-\tfrac{8}{27}(N+2)(N+8)\times[-21+12\pi^2+128\ln\tfrac{3}{4}+144\mathrm{Li}_2(-\tfrac{1}{3})]u^3, \tag{C10}$$

where we used Eq. (14). Contrary to Eq. (C9) which is well behaved regarding strong-coupling theory, Eq. (C10), which coincides with the numerical coefficients $c_m^{(2)}$ of Table 4 of [55], is problematic when considering the Borel resummation scheme: All its coefficients are negative. For this reason, we have not been able to reproduce the Borel resummation made in Ref. [55]. We shall, however, make, in the main text, a comparison between the strong-coupling limit of Eq. (C9) and the resummation performed in [55].

## APPENDIX D: THREE-LOOP AMPLITUDE FUNCTION OF THE $N=1$-SUSCEPTIBILITY BELOW $T_C$

In Ref. [40], the amplitude function of the susceptibility below $T_c$ for $N=1$ has been calculated numerically to five loops. We have quoted in Eq. (91) the corresponding two-loop part. This amplitude function enters the ratio of the susceptibilities (105). Since $f_{\chi_+}$ has been obtained to three loops in the previous section, it is also interesting to obtain $f_{\chi_-}$ analytically: The ratio (105) will thus be analytical.

In Ref. [42], the free energy $\Gamma_B$ has been given analytically up to three loops. We shall use this knowledge to determine $f_{\chi_-}$. We have recalled the relevant equations in the first part of this Appendix, which have to be evaluated for $N=1$ and $\overline{\omega}=0$. The derivative of the free energy with respect to the magnetization leads to the equation of state (B10) that can be inverted to obtain the magnetization [42]. We have recalled its expression in Eq. (B11). The equation of state can itself be derived with respect to the magnetization, defining the inverse susceptibility below $T_c$: $\chi_{-,B}^{-1}=\partial h_B/\partial M_B$. Only at this stage is the external field $h_B$ taken to be vanishing. The length $\xi_-$ [42], which we recalled in Eq. (B12), is then used to remove the nonanalyticity coming from logarithms of the coupling constant. Doing so, and using the magnetization given by the equation of state, we have been able to obtain the inverse bare susceptibility below $T_c$: $\chi_{-,B}^{-1}=\xi_-^{-2}f_{\chi_-}^B$, with

$$f^{B}_{\chi_-}=1+\frac{9}{2\pi}(u_B\xi_-)-\frac{1061}{36\pi^2}(u_B\xi_-)^2+[19\,472-11\,664c_1+3\pi^2+10\,480\ln\tfrac{4}{3}+36\mathrm{Li}_2(-\tfrac{1}{3})]\frac{(u_B\xi_-)^3}{64\pi^3}. \tag{D1}$$

Numerically, this expansion reads

$$1+1.432\,39(u_B\xi_-)-2.986\,16(u_B\xi_-)^2+11.2134(u_B\xi_-)^3. \tag{D2}$$

This result agrees perfectly with the numerical expansion given in the last column of Table 2 in [40]. Using the relation (14) between $u_B$ and $\bar{u}_B$, we obtain

$$f^{B}_{\chi_-}=1+18\bar{u}_B-\frac{4244}{9}\bar{u}_B^2+[194\,72-116\,64c_1+3\pi^2+104\,80\ln\tfrac{4}{3}+36\mathrm{Li}_2(-\tfrac{1}{3})]\bar{u}_B^3. \tag{D3}$$

The renormalized version of Eq. (D3) is found by multiplying it with $Z_\phi$ from Eq. (16):

$$f_{\chi_-}=1+18\bar{u}_B-\frac{4352}{9}\bar{u}_B^2+[199\,04-116\,64c_1+3\pi^2+104\,80\ln\tfrac{4}{3}+36\mathrm{Li}_2(-\tfrac{1}{3})]\bar{u}_B^3. \tag{D4}$$

This is the amplitude to be evaluated in the strong-coupling limit and entering the ratio (105).

The bare amplitudes (C8) and (D3) might as well be chosen to enter the amplitude ratio (105) since the renormalization constant $Z_\phi$ drops out, being the same above and below $T_c$. We have, however, chosen to work with the renormalized quantities (C9) and (D4).

For completeness, we also state the expansion of $f_{\chi_-}$ in terms of the renormalized coupling constant. Using Eqs. (14) and (D4), we obtain

$$f_{\chi_-}=1+18u+\frac{1480}{9}u^2+[1072-116\,64c_1+3\pi^2+104\,80\ln\tfrac{4}{3}+36\mathrm{Li}_2(-\tfrac{1}{3})]u^3. \tag{D5}$$

Taking the inverse of this equation, we recover the coefficients of the second column of Table 3 of Ref. [40].

For an application to the evaluation of the amplitude ratio of the susceptibilities, we also give the perturbative expansion of the ratio $f_{\chi_-}/f_{\chi_+}$ at $N=1$. Combining Eq. (C9) with Eq. (D4), we obtain

$$\frac{f_{\chi_-}}{f_{\chi_+}}=1+18\bar{u}_B-\frac{1420}{3}\bar{u}_B^2+[191\,84-116\,64c_1+99\pi^2+9456\ln\tfrac{4}{3}+1188\mathrm{Li}_2(-\tfrac{1}{3})]\bar{u}_B^3. \tag{D6}$$

## APPENDIX E: AMPLITUDE RATIOS

To get the different amplitude ratios of Sec. IV B, we make use of the relations

$$\chi_+=Z_\phi\frac{\xi_+^2}{f_{\chi_+}}\exp\left[-\int_{u(l_+)}^{u}\frac{\gamma_\phi}{\beta_u}du'\right], \tag{E1}$$

$$\chi_-=Z_\phi\frac{\xi_-^2}{f_{\chi_-}}\exp\left[-\int_{u(l_-)}^{u}\frac{\gamma_\phi}{\beta_u}du'\right], \tag{E2}$$

$$A^{\pm}=\frac{(b^{\pm})^2}{(\xi^0_{\pm})^D}\frac{A_D}{4}(4\nu B^*+\alpha F^*_{\pm}), \tag{E3}$$

$$\langle\phi_B\rangle^2=Z_\phi\frac{f_\phi}{\xi_-^{D-2}}\exp\left[-\int_{u(l_-)}^{u}\frac{\gamma_\phi}{\beta_u}du'\right], \tag{E4}$$

which were derived in [37] for Eq. (E1), [40] for Eqs. (E2) and (E4), and [38] for Eq. (E3). All the quantities have been defined in the main text, except for

$$l_\pm=\exp\left(\int_u^{u(l_\pm)}\frac{du'}{\beta_u}\right), \tag{E5}$$

with $u(1)=l_\pm$ and the flow parameter chosen as $l_\pm\mu\xi_\pm=1$, and with $\xi_\pm=\xi^0_\pm|t|^{-\nu}$.

The amplitude ratio of the heat capacity (100) follows trivially from Eq. (E3), while the amplitude ratio for the susceptibilities (105) is a direct consequence of Eqs. (E1) and (E2). The only missing information is the ratio $\xi^0_+/\xi^0_-$, given explicitly in [38] as

$$\frac{\xi^0_+}{\xi^0_-}=\left(\frac{b^+}{b^-}\right)^\nu. \tag{E6}$$

Because our derivation (104) of the universal combination $R_C$ does not coincide with Eq. (103) derived by the authors of [42], we reproduce below our calculation. We need the amplitude $A_M$, related to Eq. (E4) by [56] $\langle\phi_B\rangle\equiv M_B\approx A_M|t|^\beta$. We deduce

$$A_M^2=Z_\phi\frac{f_\phi}{(\xi^0_-)^{(D-2)}}|t|^{\nu(D-2)-2\beta}\exp\left[-\int_{u(l_-)}^{u}\frac{\gamma_\phi}{\beta_u}\right]\Bigg|_{l_-\to0}, \tag{E7}$$

where we have specified that the right-hand-side is evaluated at the critical point.

In the same way, the amplitude of the susceptibility is obtained from Eq. (E1) using [56] $\chi_+\approx\Gamma^+|t|^{-\gamma}$. We deduce

$$\Gamma^+=Z_\phi\frac{(\xi^0_+)^2}{f_{\chi_+}}|t|^{\gamma-2\nu}\exp\left[-\int_{u(l_+)}^{u}\frac{\gamma_\phi}{\beta_u}\right]\Bigg|_{l_+\to0}. \tag{E8}$$

Taking the ratio $\Gamma^+/A_M^2$, we have directly

$$\frac{\Gamma^+}{A_M^2} = \frac{(\xi_+^0)^2}{f_{\chi_+}^* f_\phi^*} (\xi_-^0)^{(D-2)}. \tag{E9}$$

The dependence in $|t|$ has disappeared, as it should, due to the identity $\gamma - 2\nu + 2\beta - \nu(D-2) = 0$.

Combining with the definition of $A^+$ in Eq. (E3), we get

$$R_C \equiv \frac{\Gamma^+ A^+}{A_M^2} = \frac{(b^+)^2}{f_{\chi_+}^* f_\phi^*} \left( \frac{\xi_-^0}{\xi_+^0} \right)^{(D-2)} \frac{A_D}{4} (4\nu B^* + \alpha F_\pm^*)$$

$$= \frac{(b^+)^{2-\nu(D-2)}}{(b^-)^{-\nu(D-2)}} \frac{A_D}{4} (4\nu B^* + \alpha F_\pm^*) \frac{1}{f_{\chi_+}^* f_\phi^*}. \tag{E10}$$

where we used Eq. (E6) to obtain the last equality. Using $b^+ = 2\nu P_+$ and $b^- = 3/2 - 2\nu P_+$ [38], as well as $A_3 = 1/(4\pi)$ from Eq. (8), we arrive to the amplitude ratio $R_C$ given in Eq. (104).

## APPENDIX F: DETERMINATION OF THE POLYNOMIAL $P_+$ TO THREE LOOPS

In this section, we want to derive the analytical expression for the polynomial $P_+$ up to three loops. It has been given numerically, and resummed, for $N=1,2,3$ up to five loops in [55], so that our analytical result will have to match this reference. Above $T_c$, the relation between $m'^2_B$ and the correlation length has been given in Eq. (C7) at the three-loop level. A polynomial $P_+^B$ in powers of $u_B$ is defined through the relation

$$P_+^B = \partial m'^2_B / \partial \xi_+^{-2}, \tag{F1}$$

leading to

$$P_+^B = 1 + \frac{N+2}{2\pi}(u_B\xi_+) - \frac{N+2}{\pi^2}(u_B\xi_+)^2 + \frac{N+2}{108\pi^3} \times \left[ -3(3N+22) + 12(N+8)\pi^2 + 2(43N+182)\ln\frac{3}{4} + 144(N+8)\mathrm{Li}_2\left(-\frac{1}{3}\right) \right] (u_B\xi_+)^3. \tag{F2}$$

The numeric coefficient $b_m$ of Table 2 of [55] coincides perfectly, up to three loops, with our analytical expression, which has the advantage of being valid for all $N$. Its renormalized counterpart is defined by

$$P_+ = Z_r^{-1} P_+^B, \tag{F3}$$

where the renormalization constant $Z_r^{-1}$ has been given to three loops in Eq. (15). The corresponding power series in $\overline{u}_B$ follows readily:

$$P_+ = 1 - 2(N+2)\overline{u}_B + 4(N+2)(2N+17)\overline{u}_B^2 + \tfrac{8}{27}(N+2) \times [-3(36N^2 + 837N + 3920) + 24(N+8)\pi^2 + 4(43N+182)\ln\tfrac{3}{4} + 288(N+8)\mathrm{Li}_2(-\tfrac{1}{3})]\overline{u}_B^3, \tag{F4}$$

where we have used the relation between $u_B$ and $\overline{u}_B$ given in Eq. (13), the scale $\mu$ being identified with the inverse of the correlation length: $\overline{u}_B = u_B \xi_+ A_3$. Equation (F4) is the polynomial whose strong-coupling expansion has to be calculated. The corresponding power series in the renormalized coupling constant $u$ follows from Eq. (14):

$$P_+ = 1 - 2(N+2)u + 4(N+2)u^2 + \tfrac{8}{27}(N+2)[-3(63N + 572) + 24(N+8)\pi^2 + 4(43N+182)\ln\tfrac{3}{4} + 288(N+8)\mathrm{Li}_2(-\tfrac{1}{3})]u^3. \tag{F5}$$

The reader can verify that the analytical result coincide, for $N=1,2,3$, with the numerical values in Table 4 of Ref. [55]. It differs only in the fifth decimal place of the cubic term $c_{P3}$ of this table.


[1] H. Kleinert, *Path Integrals in Quantum Mechanics, Statistics and Polymer Physics* (World Scientific, Singapore, 1995). Variational perturbation theory is developed in Chaps. 5 and 17.

[2] H. Kleinert, Phys. Rev. D **57**, 2264 (1998); **58**, 107702 (Addendum) (1998).

[3] H. Kleinert, Phys. Rev. D **60**, 085001 (1999).

[4] F. Jasch and H. Kleinert, cond-mat/9906246.

[5] H. Kleinert, Phys. Lett. B **434**, 74 (1998); **463**, 69 (1999).

[6] H. Kleinert and V. Shulte-Frohlinde, cond-mat/9907214.

[7] K. Wilson, Phys. Rev. B **4**, 3174 (1971).

[8] K. Wilson and M. Fisher, Phys. Rev. Lett. **28**, 240 (1972); K. Wilson, *ibid.* **28**, 548 (1972).

[9] E. Brézin, J. C. Le Guillou, and J. Zinn-Justin, in *Phase Transition and Critical Phenomana*, edited by C. Domb and M. S. Green (Academic Press, New York, 1976), Vol. 6, p. 125.

[10] L. N. Lipatov, *Leningrad Nuclear Physics Institute Report, 1976* (unpublished).

[11] E. Brézin, J. C. Le Guillou, and J. Zinn-Justin, Phys. Rev. D **15**, 1544 (1977); **15**, 1558 (1977).

[12] J. Zinn-Justin, *Quantum Field Theory and Critical Phenomena*, Oxford Science Publications, 3rd ed. (Oxford University Press, Oxford, 1996).

[13] H. Kleinert and V. Schulte-Frohlinde, *Critical Properties of $\phi^4$ Theories* (World Scientific, Singapore, 2001), http://www.physik.fu-berlin.de/~kleinert/b8.

[14] K. G. Chetyrkin, S. G. Gorishny, S. A. Larin, and F. V. Tkachov, Phys. Lett. **132B**, 351 (1983).

[15] H. Kleinert, J. Neu, V. Schulte-Frohlinde, K. G. Chetkyrin, and S. A. Larin, Phys. Lett. **272B**, 39 (1991); Phys. Lett. **319B**, 545(E) (1993).

[16] D. I. Kazakov and D. V. Shirkov, Fortschr. Phys. **28**, 465

(1980); J. Zinn-Justin, Phys. Rep. **70**, 3 (1981); **70**, 109 (1981).
[17] J. C. Le Guillou and J. Zinn-Justin, J. Phys. (France) Lett. **46**, L137 (1985); J. Phys. (Paris) **48**, 19 (1987).
[18] R. Guida and J. Zinn-Justin, J. Phys. A **31**, 8103 (1998); e-print cond-mat/9803240. See also J. Zinn-Justin, e-print hep-th/0002136.
[19] G. Parisi, J. Stat. Phys. **23**, 49 (1980).
[20] G. A. Baker, B. G. Nickel, M. S. Green, and D. I. Meiron, Phys. Rev. Lett. **36**, 1351 (1976); B. G. Nickel, D. I. Meiron and G. A. Backer, University of Guelph report, 1977 (unpublished); G. A. Baker, B. G. Nickel, and D. I. Meiron, Phys. Rev. B **17**, 1365 (1978).
[21] R. Guida and J. Zinn-Justin, Nucl. Phys. B **489**, 626 (1997).
[22] G. Münster and J. Heitger, Nucl. Phys. B **424**, 582 (1994).
[23] C. Gutsfeld, J. Kuüster, and G. Münster, Nucl. Phys. B **479**, 654 (1996).
[24] C. Bagnuls and C. Bervillier, Phys. Rev. B **32**, 7209 (1985).
[25] C. Bagnuls, C. Bervillier, D. I. Meiron, and B. G. Nickel, Phys. Rev. B **35**, 3585 (1987).
[26] P. C. Hohenberg, A. Aharony, B. I. Halperin, and E. D. Siggia, Phys. Rev. B **13**, 2986 (1976).
[27] C. Bervillier, Phys. Rev. B **14**, 4964 (1976).
[28] J. A. Lipa, D. R. Swanson, J. A. Nissen, T. C. P. Chui, and U. E. Israelsson, Phys. Rev. Lett. **76**, 944 (1996); J. A. Lipa, D. R. Swanson, J. A. Nissen, Z. K. Geng, P. R. Williamson, D. A. Stricker, T. C. P. Chui, U. E. Israelsson, and M. Larson, *ibid.* **84**, 4894 (2000). In the second paper, the value of $\alpha$ given in the first paper was corrected to $\alpha = -0.010\,56 \pm 0.0004$.
[29] The presence and origin of confluent singular terms have been first understood from renormalization group analysis by F. J. Wegner, Phys. Rev. B **5**, 4529 (1972). For a determination of the critical behavior of the first confluent singular term for the specific heat to the order $\epsilon^2$, see M.-C. Chang and A. Houghton, *ibid.* **21**, 1881 (1980) (The ratio of the leading amplitude ratio for the heat capacity is incorrect in this later reference, as it is in [27]. For the corrected value for $N=1$, see [31], which also gives other various confluent terms and gives references to other wrong ratios in the literature. For the corrected value of $A^+/A^-$ for all $N$, see C. Bervillier, *ibid.* **34**, 8141 (1986), or Appendix C of Ref. [25].)
[30] C. Bagnuls and C. Bervillier, Phys. Rev. B **24**, 1226 (1981).
[31] J. F. Nicoll and P. C. Albright, Phys. Rev. B **31**, 4576 (1985).
[32] G. M. Avdeeva and A. A. Migdal, Pis'ma Zh. Éksp. Teor. Fiz. **16**, 253 (1972) [JETP Lett. **16**, 178 (1972)]; E. Brézin, D. J. Wallace, and K. G. Wilson, Phys. Rev. Lett. **29**, 591 (1972); Phys. Rev. B **7**, 232 (1972).
[33] D. J. Wallace and R. K. P. Zia, Phys. Lett. **46A**, 261 (1973); J. Phys. C **7**, 3480 (1974).
[34] C. Bervillier and M. Shpot, Phys. Rev. B **46**, 955 (1992).
[35] A. R. Rajantie, Nucl. Phys. B **480**, 729 (1996); **513**, 761 (Addendum) (1998).
[36] V. Dohm, Z. Phys. B: Condens. Matter **60**, 61 (1985).
[37] R. Schloms and V. Dohm, Nucl. Phys. B **328**, 639 (1989).
[38] R. Schloms and V. Dohm, Phys. Rev. B **42**, 6142 (1990); **46**, 5883 (Addendum) (1992).
[39] See Chang and Houghton in Ref. [29].
[40] F. J. Halfkann and V. Dohm, Z. Phys. B: Condens. Matter **89**, 79 (1992).
[41] S. A. Larin, M. Mönnigmann, M. Strösser, and V. Dohm, Phys. Rev. B **58**, 3394 (1998).
[42] M. Strösser, L. A. Larin, and V. Dohm, Nucl. Phys. B **540**, 654 (1999).
[43] B. Kastening, Phys. Rev. D **57**, 3567 (1998).
[44] J. C. Le Guillou and J. Zinn-Justin, Phys. Rev. B **21**, 3976 (1985).
[45] H. KLeinert and B. Van den Bossche (unpublished).
[46] S. S. C. Burnett, M. Strösser and V. Dohm, Nucl. Phys. B **504**, 665 (1997); **509**, 729 (Addendum) (1998).
[47] J. S. Kang, Phys. Rev. D **13**, 851 (1976).
[48] H. Kleinert and B. Van den Bossche (unpublished).
[49] H. Kleinert, Phys. Lett. B **463**, 69 (1999).
[50] Note that the calculation we do in this paper are based on the normalization of the coupling constant of Dohm and coworkers [42,41,46] which differ from Kleinert's [5,13]. The difference in conventions disappears at the level of the exponents, and the value of $u^*$ is only different by a factor 12, as mentioned after Eq. (11).
[51] B. Li, N. Madras, and A. D. Sokal, J. Stat. Phys. **80**, 661 (1995).
[52] S. A. Antonenko and A. I. Sokolov, Phys. Rev. E **51**, 1894 (1995).
[53] M. E. Fisher, M. N. Barber, and D. Jasnow, Phys. Rev. A **8**, 1111 (1973).
[54] I. S. Gradshteyn and I. M. Ryzhik, *Table of Integrals, Series and Products*, 4th ed. (Academic Press, London, 1965).
[55] H. J. Krause, R. Schloms, and V. Dohm, Z. Phys. B: Condens. Matter **79**, 287 (1990); **80**, 313 (Addendum) (1990).
[56] V. Privman, P. C. Hohenberg and A. Aharony, in *Phase Transition and Critical Phenomana*, edited by C. Domb and J. L. Lebowitz (Academic Press, London, 1991), Vol. 14, p. 1, and references therein.
[57] I. D. Lawrie, J. Phys. A **14**, 2489 (1981).
[58] H. Kleinert and B. Van den Bossche (unpublished).